# WRAPPING CAM MECHANISMS

by

Paul H. Tidwell, II

Dissertation submitted to the Faculty of the

Virginia Polytechnic Institute and State University

in partial fulfillment of the requirements for the degree of

DOCTOR OF PHILOSOPHY

in

MECHANICAL ENGINEERING

APPROVED:

Charles F. Reinholtz, Chairman

Sanjay G. Dhande

Ronald W. Landgraf

Harry H. Robertshaw

William R. Saunders

August, 1995
Blacksburg, Virginia

Key Words: Cams, Cam-Mechanisms, Band-Mechanisms,
Kinematic-Synthesis, Force-Synthesis

WRAPPING CAM MECHANISMS

by

Paul H. Tidwell, II

Charles F. Reinholtz, Chairman

(ABSTRACT)

This dissertation is a treatise on "wrapping cam mechanisms." This intriguing mechanism is composed of a cam wrapped by a belt, chain, or other flexible follower. Such devices have also been referred to as band mechanisms. The flexible follower is assumed to be constrained such that there is no relative sliding between it and the cam.

This dissertation provides the first comprehensive kinematic study of wrapping cam mechanisms. Different forms of this mechanism are enumerated, and two forms believed to be of particular importance are identified. Kinematic analysis techniques are developed to determine the relative positions and internal forces in the mechanism as it moves. Kinematic synthesis methods are developed to generate the surface of a cam to produce a desired displacement or mechanical advantage. These original closed-form techniques are developed from the basic laws of conjugate geometry. While wrapping cams are far less common than cams that generate a specified follower displacement functions, applications exist in archery, counter-balancing mechanisms, exercise equipment, clamping and locking mechanisms, and process machines.

To my grandfathers:

Paul Hickman Tidwell, I
and
Howard McChesney Dobson, Sr.

# Contents

# List of Figures

# Acknowledgements

Primarily, I would like to thank my advisor Dr. Charles F. Reinholtz. He is my colleague and friend who envisioned that this work was feasible. Without his guidance and attention, it would not be possible. His dedication and integrity are truly inspirational. And, to Dr. Harry Robershaw, I am grateful for his friendship and advice.

More thanks to the engineers at Nautilus. In particular, Greg Webb and Michael A. Lo Presti are gifted engineers doing great work in the real world. Also, Nautilus and Virginia's Center for Innovative Technology should be recognized for their continuing support of this work.

Thanks to my many office mates and the rest of the graduate students at Virginia Tech. Their camaraderie and friendliness made me stay so long.

Finally, I would like to express my appreciation to my parents who told me I was smart and could make it when I failed second grade.

# Chapter 1

# Introduction

A mechanism is a device that transforms force and motion. For example, a four-bar linkage can transform the rotation of a driving shaft into the oscillation of the rocker-arm. The transformation may be just a constant change of speed, such as a gear train; or it may be more general involving complex functional relationships. This dissertation is an investigation of the wrapping cam mechanism which is capable of producing these transformations.

## 1.1 Motivation

Cam mechanisms have been important for centuries. One of the six simple machines described by Norton, the wedge or inclined plane, is a linear cam (1993). These have been used for thousands of years. Modern cam-mechanism arrangements include standard cam-follower mechanisms, cam-modulated linkages, indexing cam mechanisms, and wrapping cam mechanisms. Cams frequently have advantages over other mechanisms including low cost, exact position control, and the ability to dwell.

## 1.2 Definition of Wrapping Cam Mechanisms

A simple wrapping cam mechanism is shown in Fig. 1.1. A wrapping cam mechanism is composed of a cam wrapped by a belt or chain follower in which no sliding occurs between the cam and follower. Using this definition, wrapping cam mechanisms can be kinematically equivalent whether the cam is smooth or has teeth. Similarly, the follower can be a chain, band, belt, or cable.

The wrapping cam mechanism can also be viewed as a hybrid cam-gear mechanism.

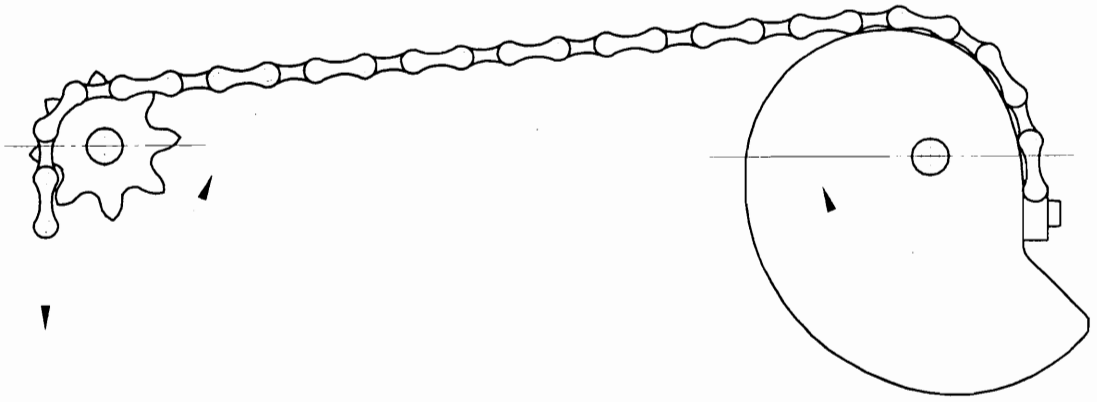

Figure 1.1: Wrapping Cam Mechanism with Chain Follower

Because there can be no sliding between the cam and follower, a kinematically similar mechanism may be constructed by replacing the belt with a rack or other rigid member. The motions of the cam and follower are the same as long as there is no relative sliding between cam and follower and the flexible member remains taut during the motion. The methods described herein may easily be applied to these "cam-rack mechanisms."

Kinematically, all embodiments of wrapping cam mechanisms are modeled using the same *pitch surface*. This theoretical surface would produce an equivalent motion if wrapped by a follower of zero thickness. As shown in Fig. 1.2, this surface is the center of the follower as it wraps the cam. The *line of connection* is the line running down the center of the belt between the cam and its support. It is tangent to the pitch surface of both the cam and pulley. The *point of contact* is the point on the cam surface where the belt is tangent to the cam surface.

In this dissertation, unless stated otherwise, all wrapping cam mechanisms will be modeled as smooth cams, and belts will be used as the wrapping followers. Other possibilities, including roller chains, have been used in successfully in many applications (Nautilus, 1993). Fig. 1.1 shows a chain to emphasize that there is no sliding between the cam and follower. Chains are typically stronger and more durable than belts. Chains only contact the cam at the discrete roller locations and can only bend at the pins connecting the individual links. This limitation introduces errors and limits the accuracy of synthesis methods (Binder, 1956). Bands are typically flexible metal belts. Wrapping cam mechanisms have also been called *band mechanisms*. Cables have also been used in wrapping cam mechanisms in exercise equipment and hunting bows (Csatari, 1994 and Browning, 1995). Cables are compact and inexpensive and allow simple implementation of three dimensional cams; however, they stuffer from fatigue, especially around small

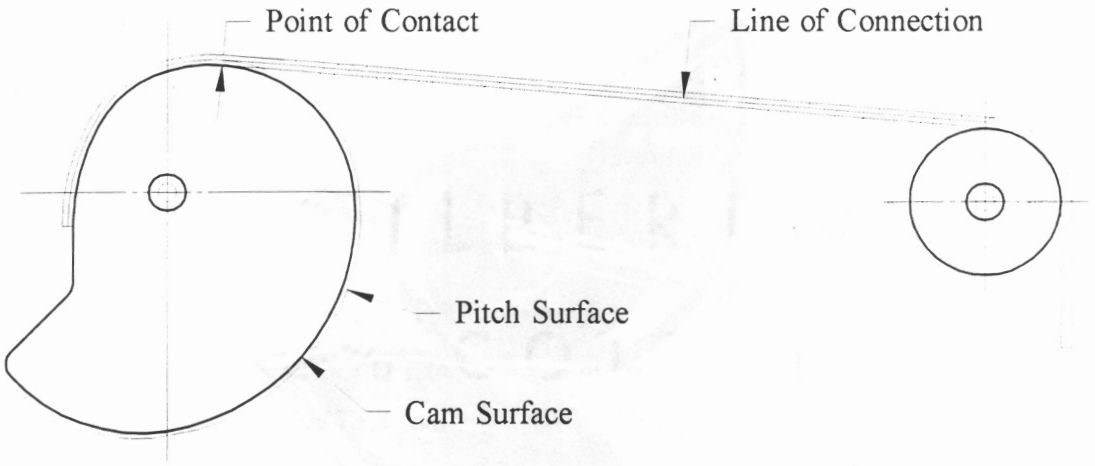


Figure 1.2: Wrapping Cam Mechanism with Belt Follower

radius bends. Rack-cam systems (toothed rigid beams meshing with toothed cams) are strong but have many disadvantages. They are expensive, heavy, and must be attached to the cam in some manner to remain in contact. These noncircular sprockets are more difficult to machine than smooth cams.

## 1.3 Mechanisms

The wrapping cam mechanism is a class of mechanisms similar to slider-crank mechanisms, and planetary-gear systems. It is another subset of planar mechanisms. The study of mechanisms may be divided into two major areas, analysis and synthesis.

Analysis is the study of existing mechanisms or mechanisms with known dimensions. Position analysis provides the location of all elements of a mechanism given the values of the independent input parameters. Velocity and acceleration analysis are used to determine the derivatives of motion at a particular position. Force analysis is used to solve for the internal forces between individual members of the mechanism. Much can be gained from kinematic analysis. Limited design may be done with analysis, by iteratively guessing the parameters that describe the mechanism and analyzing its performance.

Synthesis involves directly generating mechanisms from a given set of design requirements for a specific task. Formulating synthesis methods is more difficult. Synthesis methods have been developed to design many types of mechanisms. Although complex, methods of choosing the type of mechanism, called type synthesis, have been developed. Type synthesis involves enumeration of all possible mechanism forms that can perform a

particular task. Both analysis methods and synthesis techniques have been developed for wrapping cam mechanisms in this dissertation.

## 1.4 Approach

The approach for this study of wrapping cam mechanisms is similar to those for other mechanisms. The topics of enumeration, analysis, type synthesis, and synthesis are addressed in this dissertation.

Wrapping cam mechanisms have not been extensively studied, previously. Two mechanisms which fit into the category of wrapping cam mechanisms were known previously, but many new mechanisms are developed in this investigation. A catalog of possible wrapping cam mechanisms is produced. Significant entries are identified for further study. Analytical analysis techniques are developed for these important mechanisms. Methods for synthesis are also developed. These are closed-form analytical techniques for producing cam profiles for wrapping cam mechanisms for position (function generation) and force (mechanical advantage) requirements. Finally, experimental verification of the analysis and synthesis methods is performed to insure the accuracy of the procedures.

# Chapter 2

# Literature Review

## 2.1 Wrapping Cam Mechanisms

The Scottish engineer and physicist William J. M. Rankine, best known for his work on engine cycles, first described the wrapping cam mechanism over one hundred years ago (1893). His illustration is shown in Fig. 2.1. In this mechanism, a belt connects two pulleys, one or both of which are eccentric or non-circular. The mechanism has two gear pair connections and two revolute joints. The type of joints, labeled G and R respectively, in the mechanism are used to identify the mechanism. This "GGRR" mechanism is further studied in Sections 3.3, 4.3, and 5.4 of this dissertation. Rankine also described using two identical elliptical pulleys to vary the velocity-ratio without a belt tensioner. Rankine presented methods for analyzing the velocity-ratios between the two pulleys. This type of wrapping cam mechanism was patented for use in exercise machines (Webb, 1993). Chironis eliminated belt sag by adding a connecting plate to this mechanism which "can transfer the precise angular rotation of one shaft to another over long distances. With proper cam design, the mechanism also produces a mathematical-function rotation for a given constant input rotation" (1965, 1991). These authors do not, however, develop synthesis methods or consider other possible configurations.

Svoboda describes the use of "belt cams" in computing mechanisms (1948). In an example, a belt winds a cylinder and spirally shaped cone for use as a squaring device. He presented approximate synthesis equations and claims very high precision.

The founder of Nautilus, Arthur Jones, developed a line of exercise machines using wrapping cam mechanisms in the 60's. Although the engineers at Nautilus developed approximate graphical synthesis methods, these are proprietary and tailored to a few specific cases.

Molian presented a wrapping cam mechanism which he called a band mechanism

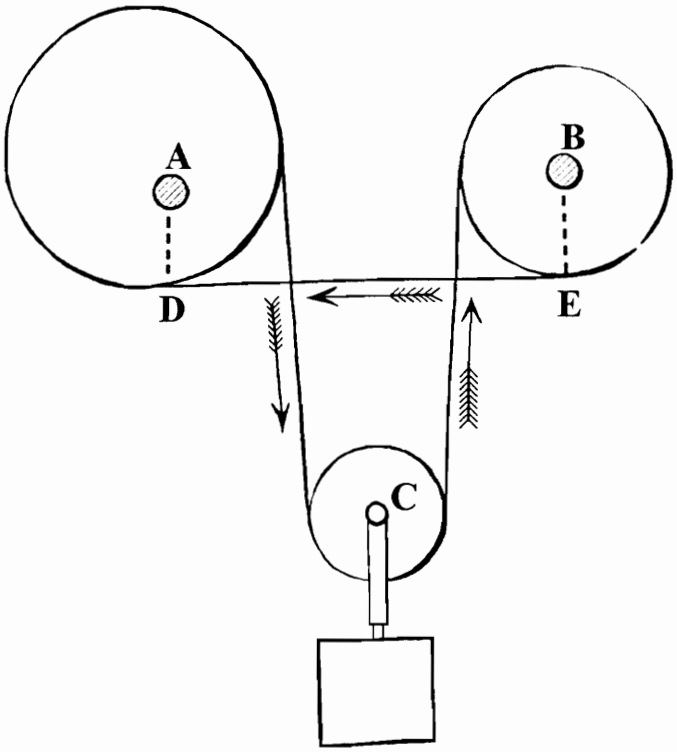


Figure 2.1: William J. M. Rankine's 1893 Wrapping Cam Mechanism with Tensioner

(1968). A belt wraps a cam and is connected to a linear spring which is anchored to the ground. This device can produce any increasing torque function. He attempts an analysis method but incorrectly calculates the length of belt wrapping on the cam.

McPhate also studied a wrapping cam mechanism (1966). This mechanism contains a cam and pulley on two parallel shafts connected by two belts such that there is no slack in the system. This mechanism has the advantage of controllable backlash. He presented an analytical synthesis technique for function generation but neglected the thickness of the belt. He also developed criteria for functions which determine if the mechanisms can be used.

Recently in Germany, Luck, and Modler developed Burmester theory for a wrapping cam mechanism for path generation (1995). Their mechanism is similar to a four-bar linkage with two links replaced by a belt and cam. The cam can be either the coupler or ground. They developed synthesis techniques using differential geometry for path generation although they neglected the thickness of the belt. They also address the case where a circular cam is used and demonstrate that a four-bar linkage is a special case of this mechanism.

Many authors have referred to wrapping cam mechanisms as band mechanisms. Band mechanisms include many belt pulley arrangements that have no cams. Wrapping cam mechanisms are really a subclass of band mechanisms. The terminology of "wrapping cam" is believed to be more descriptive and is used for this dissertation.

Wrapping cam mechanisms have not been studied as extensively as other types of mechanisms. Perhaps, this is because they do not fit neatly into the modern definition of "mechanism." Mayourian and Freudenstein defined a modern mechanism "as one in which each link is defined as a rigid body, pair-connected to at least two other links, and in which relative motion between all links is possible" (1984). The belt in a wrapping cam mechanism is not a "rigid" body. Indeed, a wrapping follower has not been considered as one of the standard cam followers. If a rack is used instead of a belt, it satisfies Mayourian and Freudenstein's definition, but the potential uses of a "rack and non-circular gear mechanism" are limited.

Reuleaux defined the six basic building blocks for mechanisms: the screw, the crank (mechanisms with revolute and prismatic pairs), the wheel (including friction and toothed wheel), the tension–compression links (belts, ropes, chains and hydraulic lines), the cam, and the ratchet (1876). The wrapping cam mechanism is a combination of the cam and the tension–compression link.

Hain categorized mechanisms into groups (1967). One category is belt mechanisms. He enumerated eight six-link belt mechanisms and established equivalency between belt mechanisms and pure-link mechanisms. In this development, he describes wrapping cam mechanisms but does not address methods for analysis or synthesis. He also mentioned that "circular pulleys can be replaced by noncircular pulleys of any desired contour, which increases the freedom available to the designer in developing the mechanism."

## 2.2 Kinematic Synthesis

Geometric graphical synthesis was originally begun by the Germans in the late nineteenth century and further developed in the first half of the twentieth. In the early 1950's, Ferdinand Freudenstein made two significant advancements. He derived analytical methods for producing linkages, and also pioneered using computer tools for their solution (Sandor, 1993). In the years that followed, synthesis methods were extended to most forms of linkages, but wrapping cam mechanisms were not discussed. Kinematic analysis techniques have been generated (Hall, 1961).

Mayourian and Freudenstein developed an atlas of all kinematic chains to aid the task

of type synthesis (1984). Using graph theory, they show that all mechanisms with up to six links possess one of 35 structures, but they do not consider belts as possible elements. Olson, Erdman, and Riley present a systematic procedure for type synthesis and review the literature for type synthesis (1985). Most type synthesis deals with linkages consisting of only revolute joints (Ananthasuresh and Kota, 1993).

## 2.3 Cam Synthesis

Synthesis methods for traditional cam follower mechanisms have been well developed (Rothbart, 1965). These methods produce cam profiles to move a follower through a prescribed motion. This can be accomplished either graphically or analytically (Mabie and Reinholtz, 1987, a). Chakraborty and Dhande developed analytical techniques for synthesizing planar and spatial cams using conjugate geometry (1977). They presented the derivations for the common two-dimensional cam-and-follower arrangements as part of a general approach using transfer matrices. Shooter, Reinholtz, and West presented the conjugate geometry method using complex vectors for use in an undergraduate class (1995). Many more works present methods for design and synthesis of common cam and follower cases but none cover wrapping cam mechanisms.

## 2.4 Cam-Modulated Linkages

Cam-modulated linkages are a combination of cams and linkages. Hartenberg and Denavit present the first examples of a linkage-modulated cam and a cam-modulated linkage and outline how to synthesize the linkage for a given cam (1964). Hain enumerated twenty-one five-link cam-modulated linkage mechanisms (1970). Huey and Dixon described additional benefits of this class of mechanism including precise accuracy and a large range of output motion (1973).

Chakraborty and Dhande used conjugate geometry to design angular motion compensators (1977). Pryor applied dyad-based conjugate geometry to cam-modulated linkage synthesis (1977, 1979). Pracht, Minotti, and Dahan developed synthesis techniques for path generation (1987).

Eventoff presented an automated graphical method for synthesizing the cam profile for a cam-modulated linkage (1992). Shooter, Tidwell, and Reinholtz used conjugate geometry to solve this problem analytically (1994). None of these works combine wrapping cams with linkages.

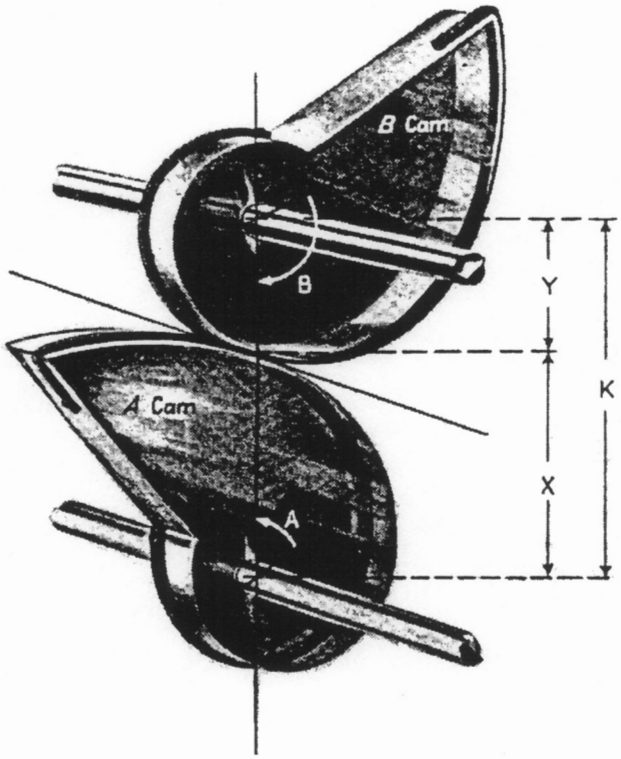


Figure 2.2: Tape Wheels or Contour Cams

## 2.5 Noncircular Gears and Contour Cams

Wrapping cam mechanisms are kinematically similar to contour cams and noncircular gears. Both contain cam-like shapes and transmit force or motion with pure rolling contact. Many different mechanisms fall into this category. These mechanisms have been used for funtion generation for many years.

Fry described the quarter squares multiplier for multiplying two inputs together mechanically (1945, a). In this mechanism, a pinion rotates on the surface of a plate on an archimedean spiral shaped path. The axis of rotation of the pinion is perpendicular to the axis of rotation of the plate.

As shown in Fig. 2.2, pairs of contour cams rotate in plane upon each other without sliding. These cams are noncircular shapes rotating on parallel shafts at a fixed distance. The cams may either have teeth or a pair of flexible bands to prevent sliding. If bands are used, each end of both bands is connected to each cam such that as one band unwraps from one cam it wraps the other cam. This mechanism is sometimes called Tape Wheels. Fry introduced synthesis methods for tape wheels (1945, b), and Yavne extended this de-

velopment (1948). His method is limited to functions that are monotonic and to cams that are convex. He also produced a method to generate cutter coordinates for manufacturing. Lockenvitz, Oliphint, and Wilde extended this development presenting methods to cut teeth into the surface of the cams (1952). Without belts, contour cams no longer need to be convex.

Noncircular gears have been used where a changing angular velocity ratio is needed and where precise nonlinear functions must be generated (Chironis, 1965). Noncircular gearing can also be used for torque balancing in planar mechanisms (Kochev, 1990).

Okada proposed a complex mechanism for producing a constant force comprising two spirally grooved, conical pulleys and a spring (1986). This contraption is a special case of a wrapping cam mechanism. It has a special geometry, and its synthesis cannot be generalized. This pulley chain arrangement is called a fusee. It is used for counteracting the diminishing torque of the uncoiling mainspring in mechanical time keeping devices. It transforms a linearly varying force into a constant force.

Harrison used a noncircular bicycle sprocket to produce nonlinear torques while studying human power output (1970). Miller and Ross developed a method for designing a noncircular bicycle sprocket for maximizing power for a given angular velocity function (1980). Freudenstein and Chen developed a chain-drive mechanism with two different noncircular sprockets (1991). This ingenious device is designed to operate without a chain tensioner. The two noncircular pulleys are designed such that there is no slack in the mechanism.

## 2.6 Force Generating Mechanisms

Some applications require a mechanism to produce a specific force instead of a motion. The fusee mechanism mentioned above is one such mechanism. Rankine described another, a simple Continuously Variable Transmission (CVT), for varying and adjusting the velocity-ratio on parallel shafts (1893). He called this arrangement speed cones. It consists of two cones or conoids connected by a belt. It is also a special case of wrapping cam mechanisms.

Four-bar linkages and springs have been used for many years to generate nonlinear forces (Goodman, 1965). Bokelberg and Gilmore used a four-bar linkage connected to a linear spring to generate a nonlinear force for exercise equipment (1989). Harmening used a torsion spring and a four-bar linkage for static mass balancing, but the techniques developed by these authors are only accurate at four positions of the mechanism (1974).

Soper et al. presented a technique for synthesizing a four-bar linkage to produce a specified resisting force or torque function (1995). Nathan has developed a constant force generator to achieve static mass balancing using a spring and a four-bar parallelogram mechanism (1985). Jo and Haug used an optimization scheme to design a single spring equilibrator (1982). Multiple linear springs have been used for "perfect" force balancing (Streit and Gilmore, 1989).

Roth presented the first formal comprehensive theory for synthesizing force-generating mechanisms (1989). Raghavan and Roth extended these concepts using screw theory for series and parallel mechanisms (1989). Huang and Roth used screw theory to synthesize spatial four-bar linkages (1994). All these methods generate mechanisms which have prescribed force characteristics only at certain precision points.

These techniques do not meet requirements for precise force generation such as those typically needed for exercise equipment. The human body is a nonlinear mechanism. For optimum exercise, the force exerted by the muscle should match its maximum potential throughout the exercise. Thus, exercise equipment should generate precise nonlinear forces. For this reason, an analytical synthesis method was developed for wrapping cams (Tidwell et al., 1992, 1994).

While other cam mechanisms have been studied extensively, general analytical analysis or synthesis techniques for wrapping cams have been largely ignored.

## 2.7 Computation and Visualization Tools

Computer tools have led to a revolution in the study of mechanisms. Kloomok and Muffley introduced the use of computers to solve cam synthesis problems on a machine capable of 9000 arithmetic operations per hour (1957).

Matlab, Mathcad, and Visual Basic are the software tools that have been used to implement the techniques developed in this dissertation. Matlab is a powerful matrix manipulation environment (1993). The first wrapping cam synthesis was implemented with it. Mathcad is a visual mathematical solving package (Mathsoft, 1994). Cam synthesis was performed with it to produce cam profiles for specific force generation problems. Visual Basic is an expanded version of the original basic computer language capable of running graphically in a Microsoft Windows environment (1993). Visual Basic is used to implement the wrapping cam synthesis tools in a simple, user-friendly package.

# Chapter 3

# Enumeration

Wrapping cam mechanisms contain a cam wrapped by a flexible belt, band, or chain. The flexible element is considered the follower. No relative sliding occurs between the cam and follower. There are many possible configurations for wrapping cam mechanisms. These can have different numbers of elements and different types of joints between the elements. Various mechanisms result depending on which link is the grounded link (inversions). Even the particular assembly of the mechanism (different branches) can effect the utility of the resulting device.

To study wrapping cams in detail, different wrapping cam mechanisms are tabulated. Eighteen distinct four-link wrapping cam mechanisms are identified. Two of these are chosen for more thorough investigation. These are the subject of later chapters on analysis and synthesis.

A directory of all possible wrapping cam mechanisms would be infinite. The list must be limited in some way. Most applications are limited to single degree of freedom solutions. Although spatial (three-dimensional) wrapping cam mechanisms are intriguing, they are less practical than 2-D devices. Enumeration of spatial linkages is also very difficult. The library developed in this dissertation will include only planar mechanisms. One of the primary advantages of wrapping cam mechanisms is their ability to be designed for continuous control of position. Simple wrapping cam mechanisms can be designed to produce exact forces or to precisely generate position functions. Designers of mechanisms composed solely of pinned links must use more complicated mechanisms to achieve more precision points. This is not necessary with wrapping cam mechanisms. Wrapping cam pairs have an infinite number of design choices. To focus on simple mechanisms the number of links is limited to four or less.

The catalog developed here will be of use to designers as they choose a mechanism to solve a specific problem. With analytical synthesis methods, it is also possible to design

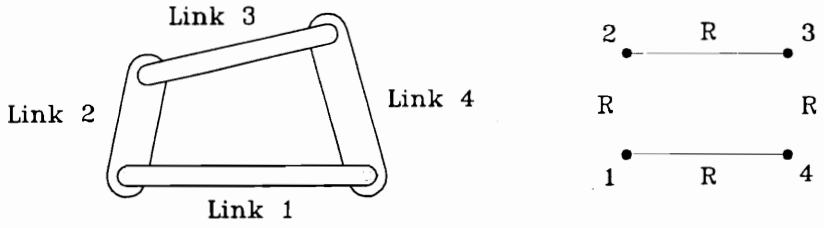


Figure 3.1: Graph of a Four-bar Linkage

several different alternatives and choose between them.

The procedure for developing the mechanisms is straightforward. First, graph theory is used to set up a framework for the search. Finding of the combinations of different possible joint types will populate the catalog of mechanisms. Using some judgment, key mechanisms are identified for further study. For these key cases, the possible choices for the ground are addressed. Finally, the effect of different assembly branches is discussed.

## 3.1 Graph Theory

Graph theory is a branch of mathematics dealing with linear graphs (formalized networks of lines connecting points). These can be represented symbolically by incidence matrices. Each link in a mechanism is a point on the graph. Each joint between two links is represented by a line between the two vertexes. For example, the four-bar linkage is a well-known single-degree-of-freedom device. As shown in Fig. 3.1, it contains four links, labeled 1 through 4. Each is connected to its two neighbors by a revolute joints, labeled "R." Its graph contains four points representing the links. Each connected to its neighbor by a line symbolizing a turning pair. All four-bar linkages are represented by the same graph shown above.

## 3.2 Wrapping Cam Mechanisms

Traditionally, only four types of joints are found in planar mechanisms. Turning pairs (R), sliding pairs (P), and gear pairs (G) each allow one degree of freedom. Wrapping cam mechanisms contain a cam and a belt with no relative sliding between them. The

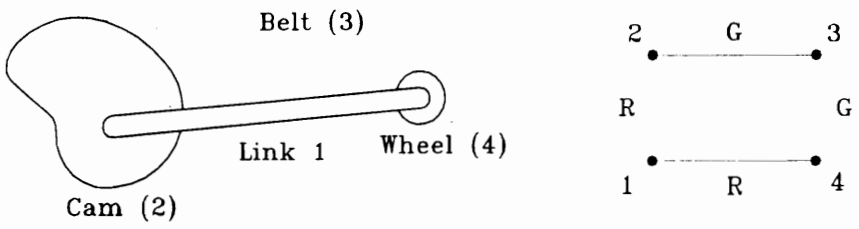


Figure 3.2: Graph of a Wrapping Cam Mechanism

traditional cam pair (C) allows sliding, while the traditional rolling contact gear pair (G) does not. Technically, therefore, the belt cam pair used in wrapping cam mechanisms is a gear pair.

Only one wrapping cam mechanism has been presented thus far. This was shown in Fig. 1.2. In this case, a belt wraps both the cam and a pulley, each of which is connected to a grounded link with revolute joints. This mechanism has four links and four single degree-of-freedom joints. The graph for it is shown in Fig. 3.2. The mechanism is labelled by the types of joints in it, and this mechanism is the GGRR mechanism.

Single degree-of-freedom mechanisms containing wrapping cam elements must have at least three links. If the mechanism has only three links and three joints, one joint must allow two degrees of freedom. Conventional cam pairs (C) permit two degrees of freedom. The other joint can be a revolute (R), prismatic (P), or gear pair (G). Because a belt can not support a moment, the free end of the belt can not connect to a prismatic joint. The very nature of a belt precludes this. If the belt connects to a traditional cam and follower set, the set must be arranged not to transmit moments to the belt. It should be mentioned that a rack does not have these limitations.

A three link wrapping cam mechanism must have a wrapping cam joint, a conventional cam joint, and a revolute, prismatic, or gear joint. With the above restrictions, there are five possible combinations of joints. The belt may connect directly to the third link with a cam pair, which connects back to the cam wrapped by the belt with either a gear, sliding, or pinned joint. The traditional cam joint may also be between wrapped cam and the third link, which connects to the belt with a revolute or gear. Let the cam be designated link 1, and the belt link 2. The belt attaches to link 3. The first joint is the wrapping cam connection between the cam and the belt. The second also connects to the belt. Examples of the five three-link mechanisms are shown in Fig. 3.3. They are labelled by the joints they possess.

All wrapping cam mechanisms with four links and one degree of freedom must have

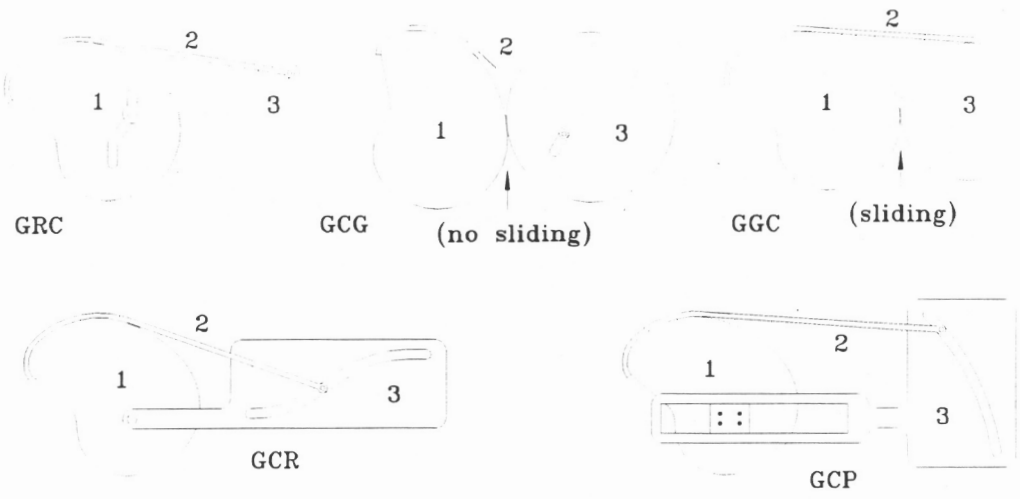


Figure 3.3: Catalog of Three-link Wrapping Cam Mechanisms

four single degree-of-freedom joints. With three possibilities (R, P, and G), there are 27 possible combinations. The mechanisms with the belt connecting to a prismatic joint must be eliminated as infeasible.

Let the cam be designated link 1, and the belt link 2. The belt attaches to link 3, and the cam to link 4. The wrapping cam pair between the first two is the first joint, and the belt connects to the second joint. With this convention established, the combinations can be enumerated. These mechanisms are illustrated in Fig. 3.4. No sliding is permitted in any of these mechanisms.

For brevity, only a few of these mechanisms will be studied in greater detail. However, the methods of detailed examination used on these are applicable to the others. Utility will be the basis for choosing configurations for further study. Useful mechanisms have an input and an output. The belt follower can not be used as an input and is a poor output, although it has been used successfully after it wraps the pulley. If a device has three or four gear pairs, more links are needed to provide the input or extract the output, although some interesting planetary gear systems may be formed if some of the gear pairs are internal. The GRRG and GRGR mechanisms also have this problem. Prismatic joints are generally less desirable because they are relatively expensive and have relatively higher friction. If the cam is mounted on a prismatic joint, the working surface i.e. the wrapped section of the cam will be small.

These restrictions leave only two practical implementations, the GGRR and GRRR. The GGRR has been the most widely used wrapping cam mechanism. Both Fig. 1.1 and 1.2 show this mechanism. The pulley arrangement is useful because either it or the free end of the belt can be used as an input or output. Kinematically, the free end is another

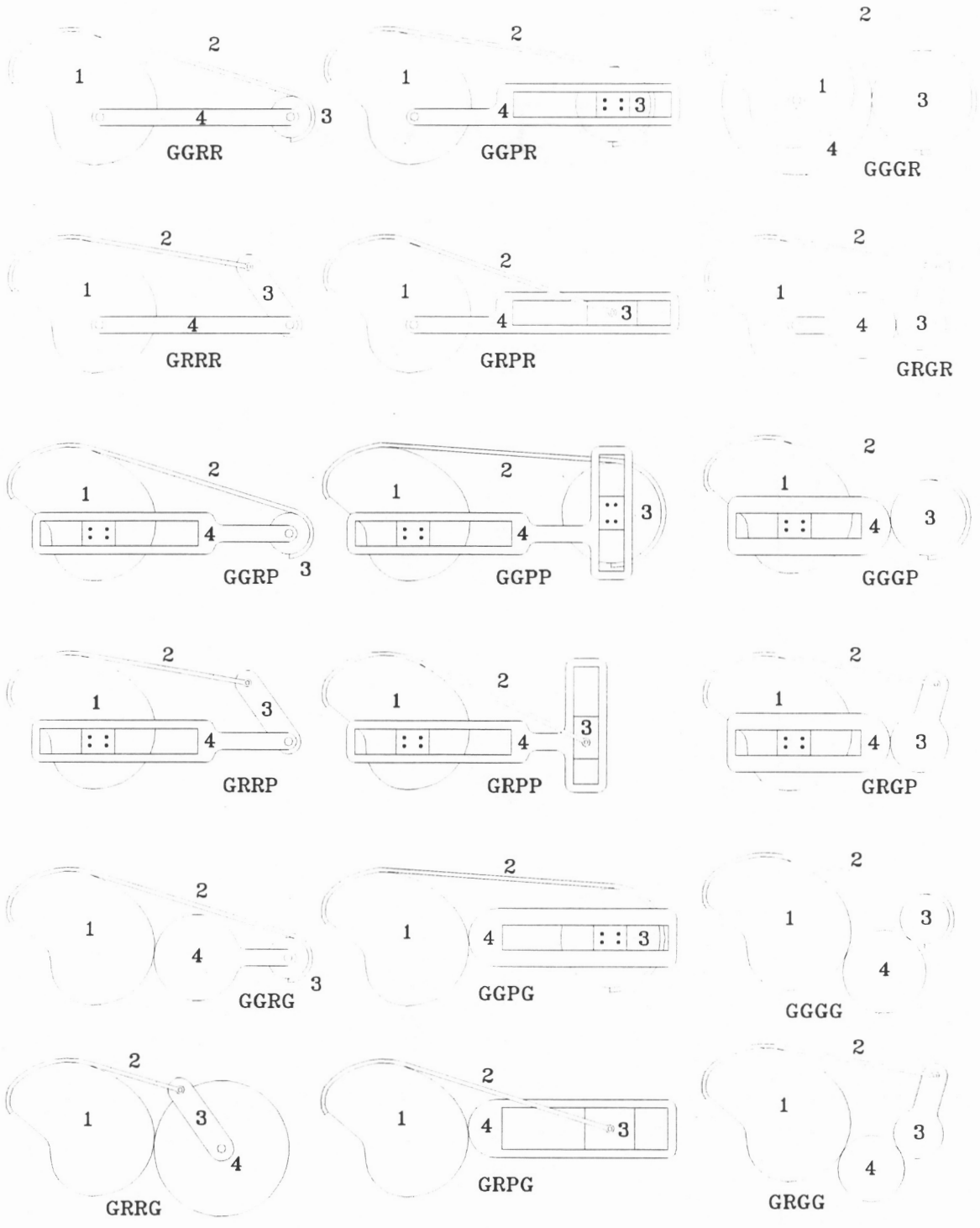


Figure 3.4: Catalog of Four-link Wrapping Cam Mechanisms

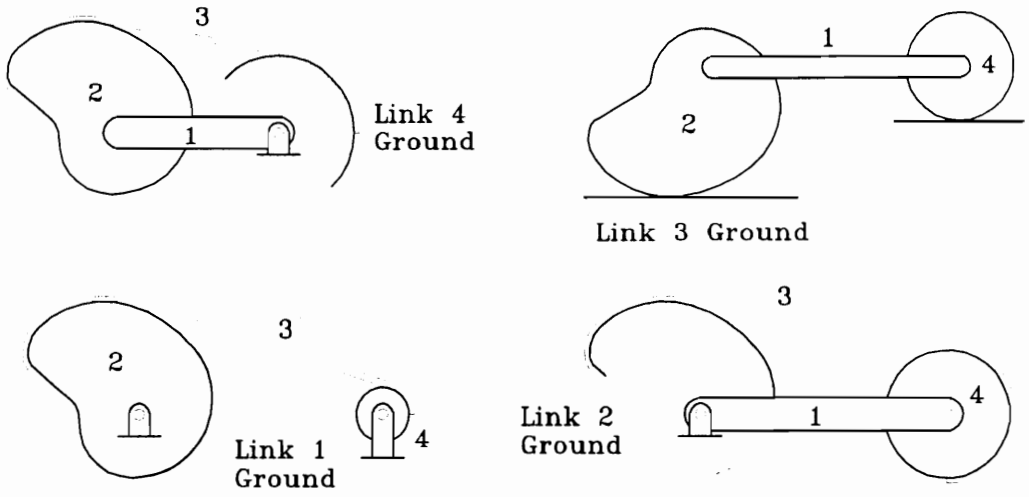


Figure 3.5: Different Grounded Links of the GGRR Mechanism

link (an input or output). Since the free end has to be secured to something, no complexity is added. The GRRR is very similar to the GGRR. The pulley and rolling contact pair of the GGRR has been replaced by a link and turning pair in the GRRR. These two mechanisms will be explored further. The methods of investigation are applicable to the other implementations of wrapping cam mechanisms.

## 3.3 GGRR Mechanism

The GGRR mechanism consists of a cam and pulley mounted to a rigid link, each connected by a revolute joint. A belt wraps both the cam and pulley. The pulley does not have to be round. It could be a noncircular gear or cam. This twist is interesting but introduces complexities. Synthesis becomes more difficult because two cams need two infinities of information to describe a solution. One noncircular surface can be defined arbitrarily and the other found through synthesis. If either cam rotates more than 360°, it must retrace the portion already used, further limiting synthesis. The mechanism with one cam and one circular pulley is generally more useful and practical. The pulley can rotate more than one revolution, and the cam can rotate up to 360 degrees.

The effect of grounding each of the links will be demonstrated. The decision of which link to connect to ground is important to the performance of the mechanism. Practical mechanisms usually have input and output links moving relative to ground. The effect of grounding each of the four members of the GRRR mechanism is shown in Fig. 3.5.

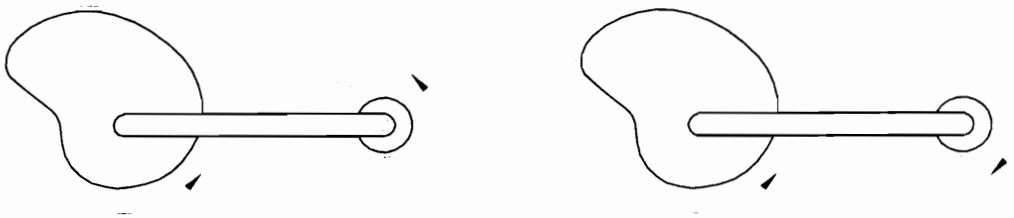

Figure 3.6: Two Branches of the GGRR Mechanism

If link 1 is grounded, both the cam and the pulley undergo simple rotation and can be used as inputs and outputs. If the cam (2) or pulley (4) is grounded, the arm (1) rotates, and the cam or pulley experiences complex rotation and translation. The belt (3) rotates but will not support a moment and is not useful as an input or output of force. This does give rise to an interesting machine. The orientation of the cam or pulley can be precisely controlled as a function of the rotation of the other. The belt itself can also be grounded. The belt does not have to be straight or even flat, but this is not a wrapping cam mechanism. The pulley and cam roll along on this surface but more links would have to be added to impart and extract any useful motion.

The most beneficial GGRR mechanism occurs with link 1 grounded. In this arrangement, the mechanism is a compact simple package. It is capable of reproducing a wide variety of nonlinear functions and providing extraordinary changes in mechanical advantage. Further study of the GGRR mechanism will focus on this case.

In addition to the choice of ground, the configuration in which the mechanism is assembled affects its performance. Specifically, there two ways (directions) the belt can wrap both the cam and pulley. The belt can cross the line between the centers of the pulley and cam, or not. This discussion will center on useful changes in the configuration not errors of assembly. As shown in Fig. 3.6, this simple change in the assembly of the device can affect the direction of relative motion and the nonlinear relationship of motion. Both of these assemblies are important. The effect of different branches will be further discussed in the chapter on synthesis.

### Racks

Even though they will generally be impractical, racks as the "wrapping element" should be mentioned for academic interest and completeness. Although some configurations are not technically wrapping cam mechanisms, they are very similar. The belt may be replaced

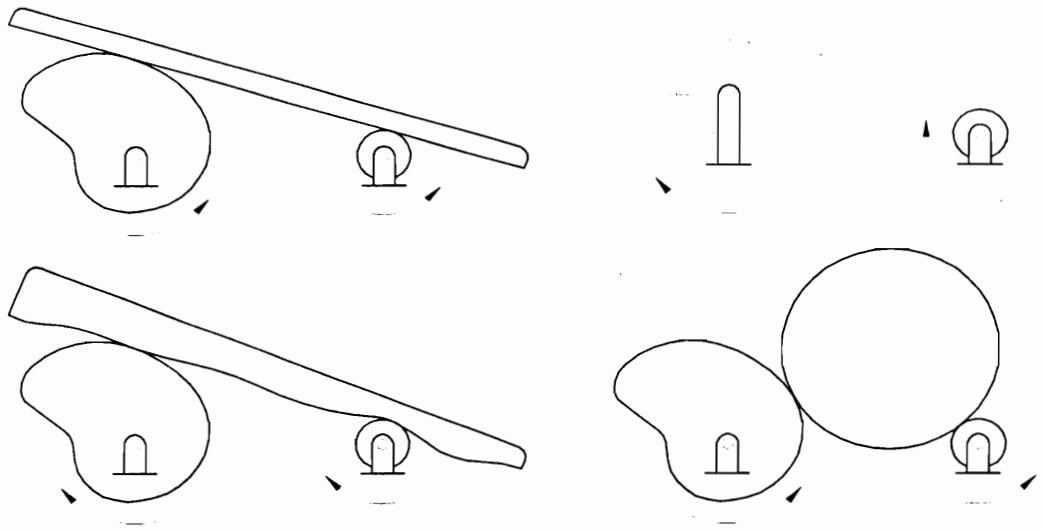

Figure 3.7: Other Rolling Contact Cam Mechanisms

with a variable thickness belt, rack, gear, or noncircular gear. Four possible replacements are shown in Fig. 3.7. The condition for these mechanisms is two rolling contact joints and two revolute joints. Just as a belt must have some tensioning mechanism, the replacement must be held in place in some manner.

The mechanism formed from a noncircular gear, a rack, and gear is an analog of the wrapping cam mechanism. The friction and mechanical connection used in wrapping cam mechanisms have been replaced by gear teeth. The same methods are used for analysis and synthesis. The rack and cam must be held together by something. For low speed and low force applications, this could be gravity. At higher speeds, another method must be used. Although unusual, the rack does not have to be straight. Analysis and synthesis become more difficult with racks of arbitrary shape, but smaller cams may be possible. Another mechanism similar to the wrapping cam mechanism is formed by replacing the rack with a gear. The gear may be noncircular, but then its center does not rotate about the second gear.

A variable thickness belt mechanism has the possible advantage of multiple revolutions of the cam but has the disadvantage that the mechanical advantage must increase with each revolution.

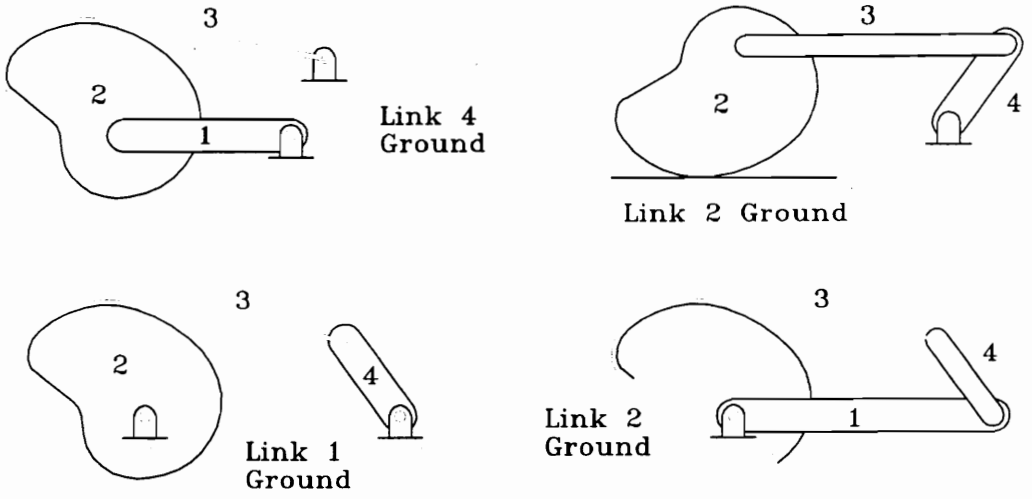


Figure 3.8: Different Grounded Links of the GRRR Mechanism

## 3.4 GRRR Mechanism

The GRRR mechanisms is mechanically as simple as the GGRR. It is constructed by replacing the pulley in the GGRR mechanism with a mechanical link and attaching the belt to the link with a revolute joint. This is a four-bar linkage with one of the link-revolute-link pairs replaced with a cam-belt-gear pair.

There is one disadvantage of this mechanism. The link, to which the belt attaches, must rotate less than 180 degrees without passing through a dead center position. The cam can rotate up to 360, and there are many useful connections to a rotating link.

As with the GGRR mechanism, any of the four links can be ground. The effect of grounding each of the four members of the GRRR mechanism is shown in Fig. 3.8. If the cam (2) or link 4 is grounded, the link 1 and belt (3) rotate, but the rotation of the belt can not be used as input or output. If the cam is grounded, link 4 could be the output. This is similar to the machine formed by grounding these links in a GGRR mechanism. The dead center limitation of the GRRR mechanism limits its utility here. When the belt is grounded, the cam undergoes complex rolling motion. The output could be its translation, but more links would need to be added to extract it. If link 1 is grounded, both the cam and the pulley undergo simple rotation and can be used as inputs and outputs. The case with link 1 as ground is the most important of these.

Different assemblies can be utilized with this mechanism. Two configurations of the GGRR mechanism are given as an illustration in Fig. 3.9. This simple change in

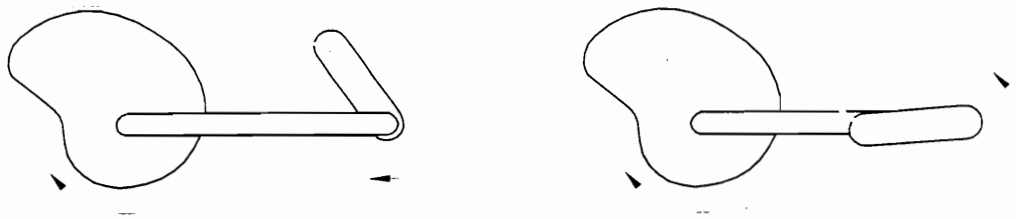

Figure 3.9: Two Different Branches of a GRRR Mechanism

the assembly of the device can effect the direction of relative motion and the nonlinear relationship of motion. The effect of different branches will be further discussed in the chapter on synthesis.

## 3.5 Type Synthesis

Of the different mechanisms enumerated, some will be better suited for some applications than others. In some cases, it will not be possible to construct a mechanism of one type.

Wrapping cam mechanisms can be used for position function generation and force generation. Different mechanisms can be used for these tasks. The range of motion desired has a large impact on the utility of these mechanisms for specific tasks.

If the application needs the same direction of rotation for the input and output, then the mechanism chosen should have an uncrossed configuration where the belt does not cross the centerline. If an opposite direction of rotation is warranted, then the mechanism chosen should have a crossed configuration where the belt crosses the centerline.

Most function generating mechanisms will have angular motion for both the input and output. Both the input and output angles have a range of values (domain). The choice of mechanism for a specific application depends on these ranges. In both the GGRR and GRRR mechanism, the cam must rotate less than one full rotation to avoid repeating part of the function. The link in the GRRR mechanism must rotate less than 180 degrees. Any rotation more than this results in the cam rotation changing direction and the belt retracing its path on the cam. There is no limit to the rotation of the pulley in the GGRR mechanism.

The designer has the freedom to choose which element is the input and which is the output, thus offering him additional flexibility. The range of rotation of the input and output provides a method for deciding which mechanism to use. A design chart of the angular ranges and possible designs is given in Fig. 3.10. This quickly eliminates some

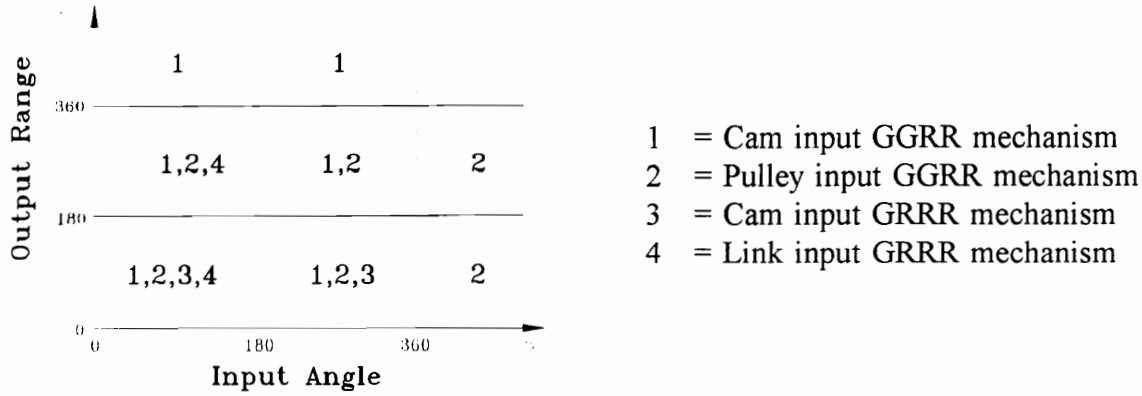


Figure 3.10: Wrapping Cam Mechanism Design Chart

mechanisms. When there is more than one mechanism for a particular application, other constraints can be used. Multiple mechanisms can be designed and the selection made based on cam profile, workspace, cost, ect.

This chart can also be used for force generation mechanisms. The angular rotation of the input and output are not arbitrary. Typically, a force generating machine produces a specified force profile as a function of output position. The domain of the input rotation is not known. It can be found using conservation of work, and Fig. 3.10 can assist the selection process.

Transmission angles must be addressed in most mechanisms. Specifically, as the angle between the arm and belt in the GRRR mechanism approaches 0° or 180°, the ability to transmit force decreases drastically. The limits on the link rotation should therefore be reduced so that the pressure angle is between 30 and 150 degrees.

## 3.6 Summary

A systematic enumeration of wrapping cam mechanisms was presented. Eighteen four-link mechanisms have been identified. Two especially useful mechanisms were selected based on kinematic constraints and design judgement. These are the GGRR and GRRR. Branch and ground choices were discussed for these. Type synthesis methods for these two were also developed. Analysis and dimensional synthesis methods for the GGRR and GRRR mechanisms are needed to utilize these mechanisms for practical applications.

This procedure can be extended to mechanisms with more than four links. There

are five different graphs with five links. These will produce 96 different wrapping cam mechanisms. There are twenty-six different topologies with six links and generating at least 570 more mechanisms.

# Chapter 4

# Analysis

To study the performance of wrapping cam mechanisms, kinematic analysis methods are needed. These methods will be used to determine the positions of all links at any input position during the motion of the mechanism. Since these mechanisms are used to generate forces, methods for static force analysis will also be developed. These analysis tools will be used to verify the synthesis methods developed in Chapter 5.

## 4.1 Approach

The analysis procedure is straightforward. All the parameters describing the dimensions of the mechanisms must be known. The wrapping cam surface profile must be described as a function having a continuous first derivative. If the surface is not known analytically, a smooth curve must be developed to approximate the discrete surface. The wrapped part of the cam, location of all revolutes, pulley diameter, link lengths, length and thickness of the belt must all be given. The follower motion is derived as it is wrapped. Geometry is used to find the motion of other elements in the mechanism as a function of the follower motion. Once the positions of the members have been found, a force analysis is performed. Assuming the elements are massless, static force balancing can be used to find the forces.

## 4.2 Cam Follower Interaction

Let the surface of the cam which touches the belt be described in polar coordinates about the pivot of the cam by a function, $p(\tau)$. If the surface is described by a series of discrete points, then an approximating polynomial can be generated by the method of least squares. The polynomial is used because it is easy to differentiate and generally provides

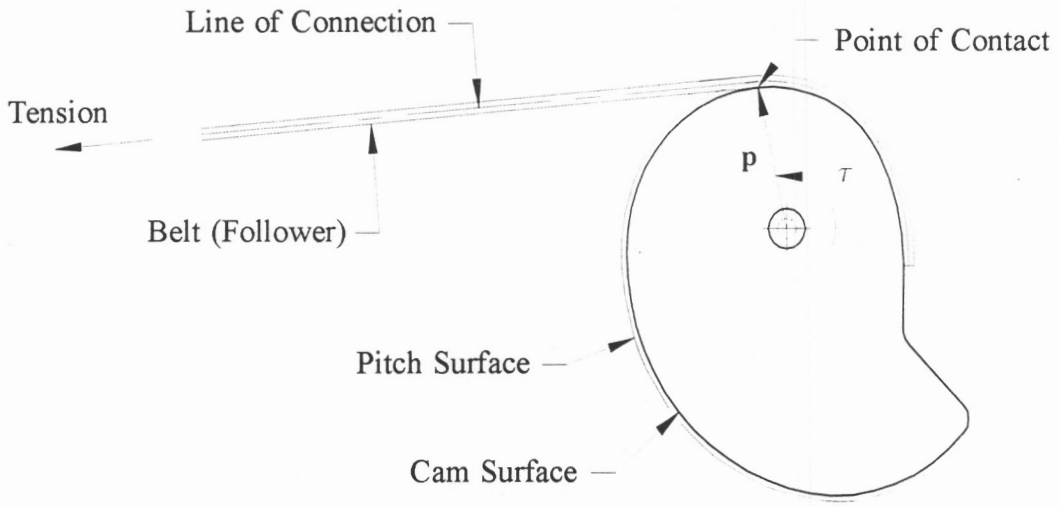


Figure 4.1: Wrapping Cam with Belt Follower

an accurate representation of the surface. Surface description can also be accomplished using intrinsic geometry, splines, Kloomok and Muffley curves (1955) or any other curves as long as the first derivative is smooth and continuous. The magnitude of this function, a scalar labeled $p$, is the distance between the cam pivot, or center, and the *point of contact* between the cam and the belt. It is a function of $\tau$, the angle locating point of contact in the cam coordinate systems shown in Fig. 4.1. This angle is measured from the contact point at the beginning of the motion cycle where the belt is fully unwrapped from the cam. The vector locating the point of contact is

$$\mathbf{p} = pe^{i\tau} \tag{4.1}$$

where $p$ is a function of $\tau$. It can be any differentiable function such as the polynomial described previously.

The *pitch surface* is the theoretical surface along the center of the belt (follower) as it wraps the cam. The *line of connection* lies along the center of the follower under tension after it leaves the surface of the cam. Let the perpendicular distance between the line of connection (tangent to the pitch surface of the cam) and the center of rotation of the cam be $h$ as shown in Fig. 4.2. The tension in the follower produces a torque on the cam through this moment arm. The value of the moment arm at the start of teh motion cycle will be designated as $h_o$.

The angle between the contact point vector, **p**, and the moment arm, $h$, is labeled $\sigma$. As the cam rotates, this angle can be found from the cam surface function, $p$. Differentiating

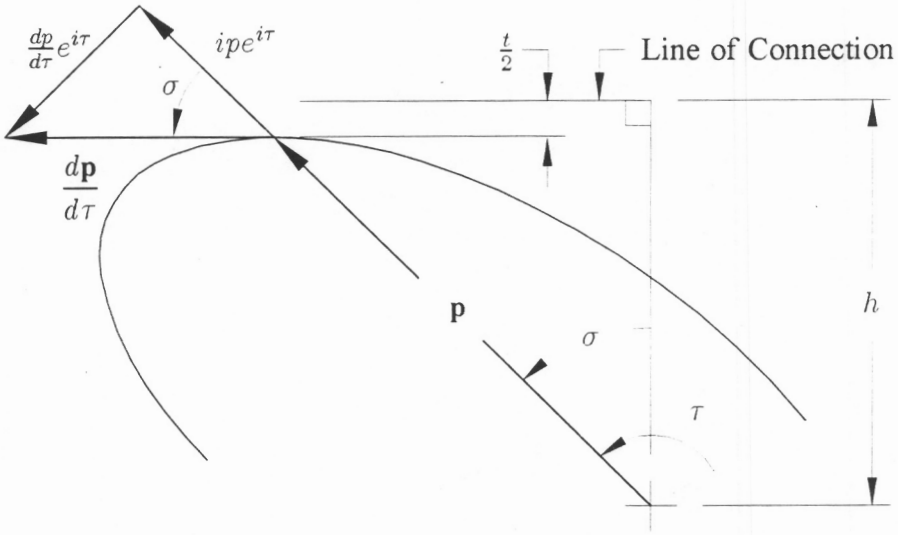


Figure 4.2: Belt Cam Interaction

equation 4.1 yields

$$\frac{d\mathbf{p}}{d\tau} = \frac{dp}{d\tau}e^{i\tau} + ipe^{i\tau} \tag{4.2}$$

This result is shown graphically in Fig. 4.2.

The angle $\sigma$ can be found directly.

$$\sigma = \tan^{-1}\left(\frac{1}{p}\frac{dp}{d\tau}\right) \tag{4.3}$$

Since $p$ is a function of $\tau$, $\frac{dp}{d\tau}$ can be found explicitly. The moment arm, $h$, can be found geometrically:

$$h = p\cos(\sigma) + \frac{t}{2} \tag{4.4}$$

where $t$ is the thickness of the belt.

Thus, the moment arm, $h$, can be found from the function describing the surface. This value is essential for position analysis and force analysis. It may seem odd that the magnitude of $h$ can be found knowing only the magnitude of $\mathbf{p}$ and its derivative and nothing about where the belt goes. For a given contact point vector $\mathbf{p}$, there are an infinite number of configurations for which there can only be one tangent and therefore only one value of $h$. For any cam, the follower motion may thus be found, but more information is needed to analyze the mechanism.

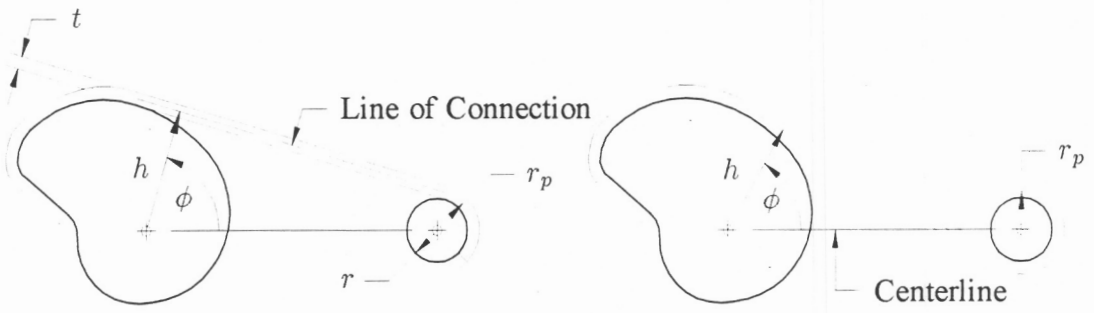


Figure 4.3: Branches GGRR Mechanism

## 4.3 GGRR Mechanism

In the GGRR mechanism, the follower wraps a pulley in addition to the cam. Let $r$ be the radius of this pulley. Let the scalar $r_p$ be defined as the pulley pitch radius, the distance from the pulley pivot to the center of the belt.

$$r_p = r + \frac{t}{2} \tag{4.5}$$

The *centerline* is the line between the center of the pulley and the pivot on the cam. The centerline has length $c$. If the belt does not cross the centerline, then the pulley and cam rotate in the same direction. If the line of connection crosses the centerline, then the pulley and cam rotate in opposite directions. This is referred to as the crossed configuration.

As shown in Fig. 4.3, let $\phi$ be the angle between the centerline and the cam moment arm, $h$. This angle can be found from the geometry. If the belt does not cross the centerline,

$$\cos(\phi) = \frac{(h - r_p)}{c} \tag{4.6}$$

If the belt does cross the centerline,

$$\cos(\phi) = \frac{(h + r_p)}{c} \tag{4.7}$$

Let cam rotation be defined by an angle $\theta$. Figure 4.4 shows the inverted mechanism with the ground link centerline rotating by the angle $\theta$. The relationship for $\theta$ is

$$\theta = \phi + \sigma + \tau \tag{4.8}$$

For convenience, $\theta$ does not start at zero but from an angle $\theta_o$, at the unwrapped (starting) position, where $\tau = 0$). The value of $\theta$ reaches a maximum at the fully wrapped position. Thus, the actual rotation of the cam from zero is $\theta - \theta_o$.

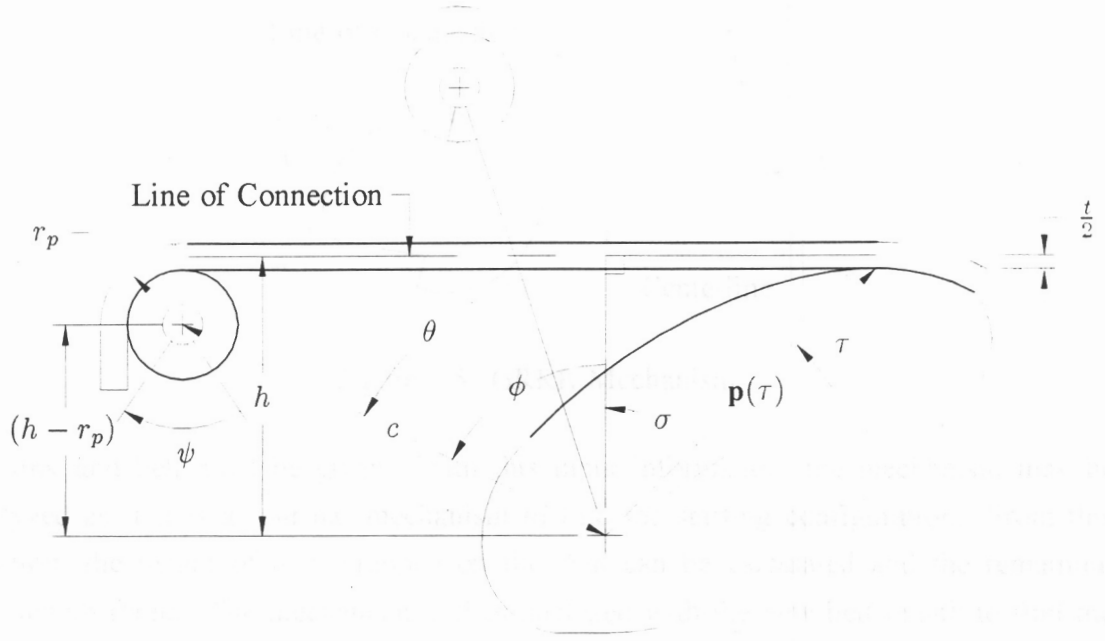


Figure 4.4: Angles in Pulley-Cam Mechanism

As the cam rotates, the pulley will also rotate, through an angle $\psi$ shown on Fig. 4.4. The angle is defined to be zero at the unwrapped position. If there is no slack in the belt, the velocity of the belt at the cam surface must equal the belt velocity at the pulley. This gives the angular velocity ratio relationship presented by Rankine (1893).

$$h\frac{d\theta}{dt} = r_p\frac{d\psi}{dt} \tag{4.9}$$

Therefore, since $\psi$ is linear

$$\int_{\theta_o}^{\theta} h d\theta_p = r_p\psi \tag{4.10}$$

The equation can be easily integrated numerically stepping around the cam surface from the starting point, $\theta_o$ to the position to be analyzed $\theta$. It can also be reduced to a form containing only the surface description function, $p$.

The differential of equation 4.8 is

$$d\theta = d\phi + d\sigma + d\tau \tag{4.11}$$

Therefore, with equation 4.4

$$\psi = \frac{1}{r_p}\left(\int_{\phi_o}^{\phi} h d\phi + \int_{\sigma_o}^{\sigma} h d\sigma + \int_{0}^{\tau} h d\tau\right) \tag{4.12}$$

This equation can be reduced further. Starting with the first term,

$$d\phi = -\left(1 - \frac{h \mp r_p}{c}\right)^{-\frac{1}{2}} \frac{dh}{c} \tag{4.13}$$

where $\left(r + \frac{t}{2}\right)$ is positive for the crossed configuration.

$$\begin{aligned} \int h d\phi &= \int \frac{-h}{\sqrt{c^2 - (h \mp r_p)}} dh \\ &= \frac{2}{3}\left(-c^2 \mp r_p - h\right)\sqrt{(-c^2 \mp r_p - h)} \end{aligned} \tag{4.14}$$

which can be evaluated directly at $h$ and $h_o$.

The belt moment arm is defined by equation 4.4. To remove $\sigma$ from this equation,

$$\cos(\sigma) = \frac{p}{\sqrt{p^2 + (\frac{dp}{d\tau})^2}} \tag{4.15}$$

and, differentiating equation 4.3

$$d\sigma = \frac{1}{1 + \left(\frac{1}{p}\frac{dp}{d\tau}\right)^2}\left(\frac{-1}{p^2}\left(\frac{dp}{d\tau}\right)^2 + \frac{1}{p}\frac{d^2p}{d\tau^2}\right) d\tau \tag{4.16}$$

Therefore,

$$\psi = \frac{1}{r_p}\left\{\int_{h_o}^{h} h d\phi + \int_0^{\tau}\left[\frac{p^2}{\sqrt{p^2 + \left(\frac{dp}{d\tau}\right)^2}} + \frac{t}{2}\right]\frac{p}{p^2 + \left(\frac{dp}{d\tau}\right)^2}\left[\frac{d^2p}{d\tau^2} - \frac{\left(\frac{dp}{d\tau}\right)^2}{p}\right] d\tau\right\} \tag{4.17}$$

For a given polynomial function, this integral may be evaluated directly after $\int_{h_o}^{h} h d\phi$ has been found from equation 4.14

The length of the belt is not needed to analyze the motion of the GGRR mechanism. If it is needed, the free length of belt between the cam and pulley can be calculated from equation 5.15 in Chapter 5. The total length of belt used by the mechanism is this free length plus the length that circulates around the pulley $\phi \times r_p$.

The forces arise in the mechanism as a result of externally applied forces. These can be found once the belt moment arm, $h$, has been found. Element masses are neglected

here but can easily be added using the method of superposition. Let $T_c$ and $T_p$ be the torques in the cam and pulley, and let $F$ be the tension in the belt.

$$T_c = \frac{h}{r_p} T_p \tag{4.18}$$

$$T_p = r_p F \tag{4.19}$$

$$F = \frac{T_p}{r_p} \tag{4.20}$$

Given any $T_c$, $T_p$, or $F$, the other two may be calculated, given the position of the mechanism.

If a sprocket and chain are used instead of a belt and pulley, the radius of the sprocket can be found from its number of teeth (Shigley, 1993).

$$r_p = \frac{p}{2 \sin\left(\frac{\pi}{N}\right)} \tag{4.21}$$

where $p$ is chain pitch and $N$ is the number of teeth.

The procedure for analyzing a function generation device is first to model the surface of the cam as a polynomial or other continuous function, $p(\tau)$ where $\tau$ is incremented over its domain. At each value of $\tau$, the cam rotation, $\theta$, is found and equation 4.10 is integrated to find $\psi$. One of these angles is the input variable, and the other is the output of the function generator. The function can be analyzed from the resulting table of $\theta$ and $\psi$.

A similar procedure is used for a force generating mechanism. After the cam surface is described by the vector, **p** values of $\tau$ are taken in succession. The output rotation and torque on the output are calculated. If the cam is the output of the mechanism, then $\theta$ and $T_c$ are evaluated. If the pulley is the output, $\psi$ and $T_p$ are found.

## 4.4 GRRR Mechanism

In the GRRR mechanism, the follower is attached to a rigid link as shown in Fig 4.5. Let $l$ be the length of this member and let $\psi$ be the angle of the link. The *centerline* is the line of length $c$ between the center of the pulley and the pivot on the link. If the belt does not cross this centerline, then the link and cam rotate in the same direction. If the line of connection crosses the centerline, then the link and cam rotate in opposite directions in the crossed configuration.

More information must be given to analyze the this mechanism. Unlike the GGRR mechanism, either the link and cam start angles, the length of belt, or the angle between

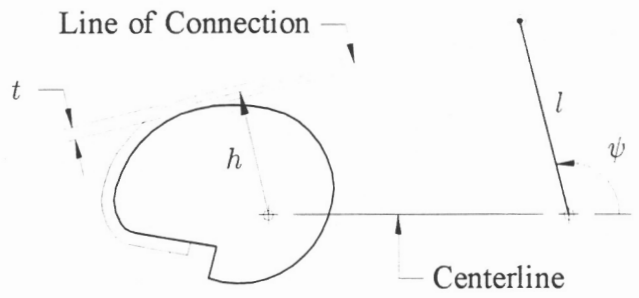


Figure 4.5: GRRR Mechanism

the link and belt must be given. With this input information, the mechanism may be analyzed as if it is a four-bar mechanism to find the starting configuration. From this position, the length of belt wrapped on the cam can be calculated and the remaining free length found. The mechanism is then analyzed with the new belt length to find the position of all the members.

As shown in Fig. 4.6, let $s_o$ be the free length of the belt at the start of motion. The subscript $o$ indicates variables at the unwrapped (start) position. Let $q_o$ be the distance between the end of the link (where the belt attaches) and the first point of contact on the cam surface. This line can be found from the belt parameters.

$$q_o = \sqrt{(s_o)^2 + \left(\frac{t}{2}\right)^2} \tag{4.22}$$

Let $\beta_o$ be the angle locating the first contact point vector $\mathbf{p}_{\tau=0}$ from the line passing through the centerline. Let $\alpha_o$ be the angle between $q_o$ and a line parallel to the centerline.

$$\alpha = \frac{\pi}{2} + \beta_o + \sigma - \tan\left(\frac{\frac{t}{2}}{s_o}\right) \tag{4.23}$$

Let $\psi_o$ be the angle between $l$ and the centerline.

Figure 4.6 looks like a four-bar linkage with $c$, $\mathbf{p}$, $q$, and $l$ as the links. The positions of these vectors can be found by solving the four-bar analysis problem. This can be easily done with complex vectors (Mabie and Reinholtz, 1987, b). Forming the vector loop equation around the equivalent four bar from the revolute connecting the link to ground

$$le^{i\psi_o} = c + pe^{i\beta_o} + q_o e^{i\alpha_o} \tag{4.24}$$

The complex conjugate of equation 4.24 results in

$$le^{-i\psi_o} = c + pe^{-i\beta_o} + q_o e^{-i\alpha_o} \tag{4.25}$$

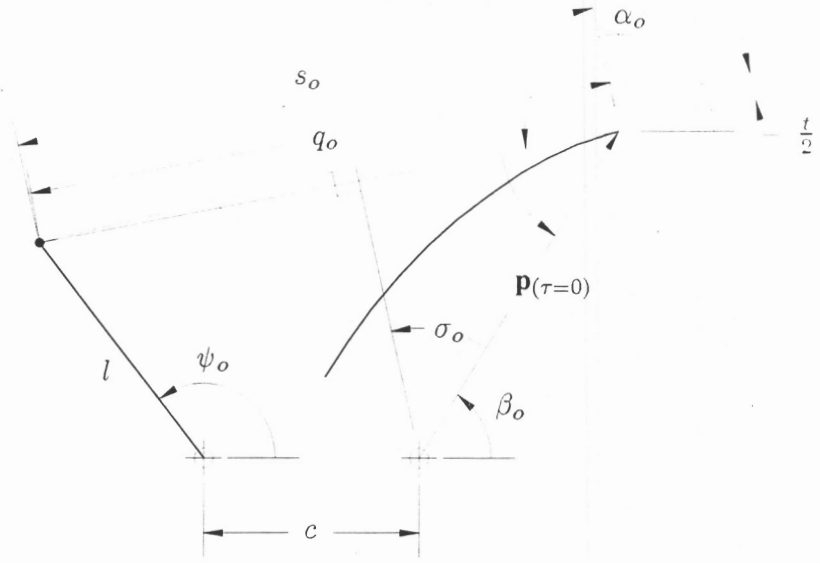


Figure 4.6: Unwrapped Position of GRRR Mechanism

Multiplying equations 4.24 and 4.25 together eliminates $\psi_o$, yielding,

$$l^2 = c^2 + p^2 + cp\left(e^{i\beta_o} + e^{-i\beta_o}\right) + cq_o\left(e^{i\alpha_o} + e^{-i\alpha_o}\right) + pq_o\left(e^{i\beta_o}e^{-i\alpha_o} + e^{-i\beta_o}e^{i\alpha_o}\right) \quad (4.26)$$

Using Euler's identity, this results in

$$l^2 = c^2 + p^2 + +q^2 + 2cp\cos\beta_o + 2cq_o\cos\alpha_o + 2pq_o\cos(\beta_o - \alpha_o) \quad (4.27)$$

This equation can be solved using the following trigonometric identities:

$$\cos\beta_o = \frac{1-t^2}{1+t^2} \quad (4.28)$$

$$\sin\beta_o = \frac{2t}{1+t^2} \quad (4.29)$$

where

$$t = \tan\frac{\beta_o}{2}$$

Substituting in these identities

$$At^2 + Bt + C = 0 \quad (4.30)$$

where

$$\begin{aligned} A &= l^2 - c^2 - q^2 - p^2 - 2cp_o - 2cq_o\cos\alpha_o + 2cp_o\cos\alpha_o \\ B &= 4q_op_o\sin\alpha_o \\ C &= l^2 - c^2 - q^2 - p^2 + 2cp_o - 2cq_o\cos\alpha_o - 2cp_o\cos\alpha_o \end{aligned}$$

The starting location for the point of contact can now be found using the quadratic formula

$$t = \frac{-B \pm \sqrt{B^2 - 4AC}}{2A} \tag{4.31}$$

One of the roots is used with the crossed configuration; the other is used with the uncrossed case. Once $\beta_o$ has been found, the other angles can be found for the starting configuration.

It is difficult to equate the velocity of the belt at the cam and the link velocity in the GRRR mechanism. The length of the belt is known. The arc length along the surface of the cam can be found (Swokowski, 1983).

$$\text{Arc length} = \int_0^\tau \sqrt{\mathbf{p}(\tau)^2 + \left(\frac{dp}{d\tau}\right)^2}\, d\tau \tag{4.32}$$

This is very close to the distance wrapped by the belt, but the true length must be measured down the center of the belt. Let $\mathbf{P}_p(\tau)$ be the vector equation describing the pitch surface of the cam (center of the wrapped belt).

$$L = \int_0^\tau \sqrt{\mathbf{P}_p(\tau)^2 + \left(\frac{d\mathbf{P}_p}{d\tau}\right)^2}\, d\tau \tag{4.33}$$

where $L$ is the length of wrapped belt.

The vector equation representing the pitch surface is

$$\mathbf{P}_p(\tau) = \mathbf{p}(\tau) + \frac{t}{2} e^{(\tau+\sigma)} \tag{4.34}$$

Differentiating yields

$$\frac{d\mathbf{P}_p}{d\tau} = \frac{d\mathbf{p}}{d\tau} + \frac{t}{2} e^{(\tau+\sigma)} \left(1 + \frac{d\sigma}{d\tau}\right) \tag{4.35}$$

$\frac{d\sigma}{d\tau}$ is found by differentiating equation 4.3.

$$\frac{d\sigma}{d\tau} = \frac{1}{1 + \left(\frac{1}{p}\frac{dp}{d\tau}\right)^2} \left(\frac{-1}{p^2}\left(\frac{dp}{d\tau}\right)^2 + \frac{1}{p}\frac{d^2p}{d\tau^2}\right) \tag{4.36}$$

Equation 4.33 can now be integrated to find the length of belt wrapped around the cam. The remaining belt length can now be found

$$s = s_o - L \tag{4.37}$$

where $s$ is the free length of the belt, and $s_o$ is total belt length from the unwrapped position.

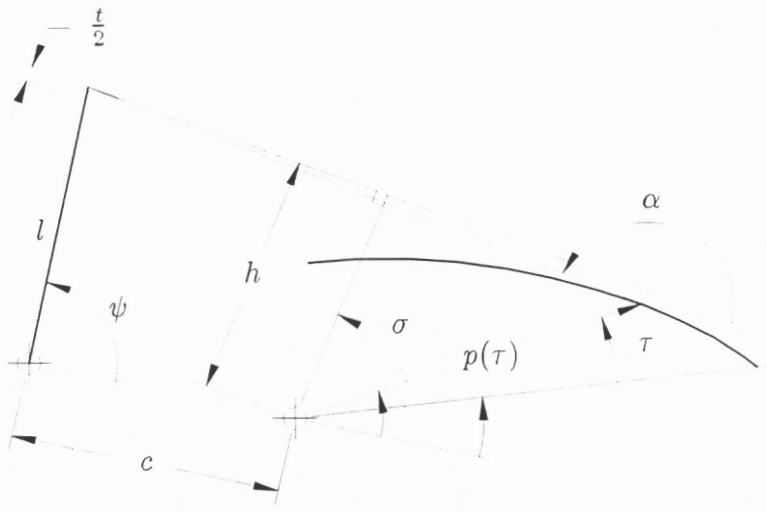


Figure 4.7: GRRR Mechanism as the Belt Is Wrapped

The mechanism is now analyzed using the same procedure as used for the starting position. The rotation of the cam, $\theta$, can now be found.

$$\theta = \beta - \tau \tag{4.38}$$

The GRRR mechanism can now be analyzed throughout its range of motion. The surface must be modelled as a smooth function, $p(\tau)$. The position of each link at the starting position is calculated. The cam angle, $\tau$, is incremented, and at each position, the amount of belt wrapped on the cam is calculated. The free length of belt is used to find the orientation of each link.

Forces arise in the mechanism as a result of externally applied forces. These can be calculated once the positions of the elements have been found. Element masses are neglected here but can easily be added using the method of super position. Let $T_c$ and $T_l$ be the torques applies to the cam and link, and let $F$ be the tension in the belt.

$$T_c = Fh \tag{4.39}$$

$$T_l = Fl\cos(\psi - \beta - \sigma) \tag{4.40}$$

$$\tag{4.41}$$

Eliminating the tension in the belts yields an expression of the torques. Given the position of the mechanism and $T_c$ or $T_l$, the other may be calculated.

$$\frac{T_c}{h} = \frac{T_l}{l\cos(\psi - \beta - \sigma)} \tag{4.42}$$

This can be done at each position of the mechanism to obtain the force response over the range of motion.

## 4.5 Convexity Requirements

The surface of the cam cannot be concave. By its very nature, the belt will only wrap convex surfaces. The analysis methods do not insure that the cam is convex. Because analysis may be performed as a check to the synthesis process, convexity requirements are included here. Simple inspection of the cam surface is the easiest way to insure convexity. It is also possible to develop analytical convexity requirements based on the cam surface description function.

The cam surface has been defined by the vector **p** locating the point of contact on the surface of the cam. This curve must be convex. Let $\kappa$ be the curvature of the curve describing the cam where $\rho_\kappa$ is the radius of curvature. At any regular point $(p, \tau)$, the curvature can be defined from the equation for $p$, in polar coordinates (Korn, 1968).

$$\kappa = \frac{1}{\rho_\kappa} = \frac{p^2 + 2\frac{dp}{d\tau} - p\frac{d^2p}{d\tau^2}}{\sqrt{p^2 + \left(\frac{dp}{d\tau}\right)^2}^3} \tag{4.43}$$

For a convex surface, the curvature must always be positive. The numerator of the above equation must, therefore, be positive. In terms of the function describing the surface, the following equality must be true to insure convexity.

$$p^2 + 2\frac{dp}{d\tau} \geq p\frac{d^2p}{d\tau^2} \tag{4.44}$$

The limitation of this analytical technique is that it indicates concavity when the origin of the coordinate system is outside the body of the cam. Good judgement is the most reliable tool in design.

## 4.6 Summary

Kinematic analysis methods have been presented for the GGRR and GRRR mechanisms. The same methods can be used to develop synthesis algorithms for other wrapping cam mechanisms enumerated in Chapter 3. Position analysis delivers the location of orientation of all of the links given a particular input parameter.

Force analysis techniques have been formulated to calculate the forces in members given an input force specification. This was accomplished assuming static conditions. Most wrapping cam mechanisms are reciprocating systems with moderate speeds. If speeds become excessive, then the belt will not be straight under tension and position

and force analysis becomes much more difficult. The same limitations are present in continuous wrapping cam mechanisms.

These analysis methods have been developed assuming all mechanism parameters are known. In many design situations, the dimensions of the mechanism are not known. Synthesis techniques are presented next to aid the designer in producing useful mechanisms.

# Chapter 5

# Kinematic Synthesis

## 5.1 Introduction

The design of mechanisms is often a difficult, iterative process. Well-developed tools for kinematic synthesis have helped to reduce the time and effort involved in developing a suitable mechanism. In linkage synthesis, the solution is usually approximate; exact motion specifications can only be met at a discrete number of precision points. Exact solutions to specified motion parameters, however, can be met with cam-based mechanisms and proper synthesis techniques. The synthesis of wrapping cams has previously been accomplished only by graphical methods. This is a time-consuming, iterative, and inexact design process. The following presentation provides a closed-form analytical method for the synthesis of wrapping cams. These synthesis techniques are used to generate cam surfaces from given performance requirements and mechanism dimensions.

Synthesis strategies for function generation synthesis and force synthesis are developed. Function generation synthesis is used to create mechanisms to produce precise angular or linear input/output relationships. Force synthesis produces cam surfaces to generate force relationships or mechanical advantages. These mechanisms will transform a given input force or torque specified as a function of input motion into a desired output force or torque function as a function of output rotation. The input force can be a constant, proportional to the input motion (linear), or nonlinear in the most general case.

## 5.2 Approach

In this chapter, closed-form expressions for the cam profiles are derived. The procedure uses the concept of conjugate geometry with classical differential geometry. The synthesis

of cams for the GGRR and GRRR mechanisms are presented as two examples of the method. The same basic techniques may be used to formulate synthesis methods for other wrapping cam mechanisms. Although the techniques developed in this dissertation are implemented only in two-dimensions, the approach is also valid for three-dimensional cam synthesis.

Cam synthesis using conjugate geometry was first presented by Chakraborty and Dhande (1977). In a cam-follower system, the surfaces of the cam and the follower must share common tangent and normal vectors. In order to maintain contact, all motion must occur along the common tangent. This is the condition of contact for the two conjugate surfaces. It states that the relative direction of the velocity of the point of contact is parallel to the tangent and therefore perpendicular to the normal to the surface. This information allows the equations of motion to be solved for the cam profile.

To aid in the development, the mechanism is inverted by fixing the cam and letting the world rotate about it. All vectors are referenced to a coordinate system attached to the fixed cam. A closed-loop vector equation is formulated within the cam and follower, locating the point of contact between the cam and follower. All of the parameters in this equation will be known except one. Determining an expression for this unknown term requires the following steps. The equation for the point of contact is differentiated with respect to the cam rotation to get an expression for the velocity of point of contact. The cam rotation in the original mechanism becomes the rotation of the ground link in the inverted mechanism. An expression for the vector normal to the cam surface is formulated. Conjugate geometry is employed by taking the dot product of the common normal and the velocity vector. Because these are perpendicular, their dot product must be zero. Setting the equation of the dot product equal to zero provides the additional information to solve the equation for the point of contact.

Some information must be supplied by the mechanism designer in the synthesis process. The purpose of the mechanism, be it function generation or production of a specified set of forces or some combination, will typically be known by the designer. The type of mechanism to perform the desired task must also be specified prior to synthesis. Some of the physical constants defining the sizes of the elements involved will be given or found from the design criteria. Synthesis methods will be developed in this chapter to produce the contour of a specified type of wrapping cam for both mechanical advantage and function generation.

If force specifications are given, the function can be integrated using conservation of work to find a differential equation between the input and output rotations. The solution

to this equation gives the functional relationship between the two rotations. Typically, the designer will know the output force as a function of the output rotation between given limits. The input force will be known as a function of the input rotation but the limits will not be known. Conservation of work will define the relationship between input and output rotation. The required forces also give the necessary length of the belt moment arm simplifying the solution. Combining these values with the condition of conjugate geometry allows the equation for the point of contact to be solved.

If a position function-generation mechanism is needed, the belt velocity can be used to generate the belt moment arm from the derivative of the given function. Once the length of the belt moment arm has been found, its orientation is derived using the geometry of the mechanism. The geometry will depend on which assembly is chosen for synthesis. The equation for the point of contact can be stated explicitly.

Detailed development of the cam synthesis method is provided below. The designer can use the methods developed here to design a specific cam to solve a specific problem. The approach for synthesizing the surface of the cam is simple once the equations for the point of contact have been found. The input motion for the mechanism is stepped through. At each position, a point on the surface of the cam is generated. This set of points describes the working surface of the cam. The set may be used directly for manufacture. If desired, the set can be used to generate a smooth curve using a technique such as cubic splines.

The cam synthesis procedure itself has been implemented on a PC using Matlab and MathCad software (1993, 1994). Once the mechanisms have been generated, they will be analyzed using the methods developed in Chapter 4 to verify the synthesis technique. These techniques have been verified experimentally.

## 5.3 Cam and Flat-faced Follower Synthesis

As shown in Fig. 5.1, if the cam is rotated through an angle, $\alpha$, an observer on the surface of the cam sees the sprocket rotating through this same angle, $\alpha$, but in the opposite sense. All vectors are referenced to a coordinate system attached to the fixed cam. This inversion will be used in much of the synthesis procedure. A closed-loop vector equation within the cam and follower is formulated to express the location of the *point of contact* between the cam and follower. If the desired motion of the follower is given, all of the parameters in this equation will be known except one. Eliminating this unknown term requires several additional steps.

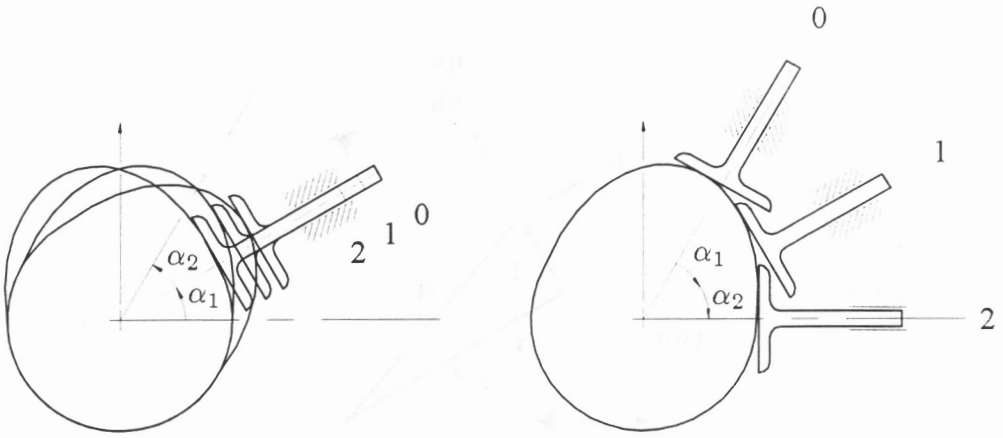


Figure 5.1: Three Positions of the Original and Inverted Mechanisms

The derivative of the vector locating the point of contact is taken with respect to the rotation of the cam to obtain an expression for the relative velocity between the cam and the follower at the point of contact. The relative velocity between the cam and the follower at the point of contact must be along the common tangent, perpendicular to the common normal. Therefore, the dot product of the common normal and the velocity vector must be zero. The unknown parameter in the vector expression for the point of contact can be found from this equation. The resulting vector expression completely describes the profile of the cam as a function of the known parameters and the cam rotation.

Use of the conjugate geometry method described above is best illustrated by a simple example. The synthesis of a disk cam with a translating flat-faced follower is well known. The derivation is presented here using complex polar notation. For the translating flat-faced follower illustrated in Fig. 5.2, let the expression $s(\theta)$ be the desired displacement of the follower. Let the angle $\theta$ describe the rotation of the cam. The vector **p** is defined as the vector locating the point on the cam in contact with the follower. The set of all points represented by **p** for a full rotation of the cam produces the cam profile. Let **r** be a vector from the cam center to the nearest point on the follower surface in the direction of the follower's motion. Note, that the magnitude of **r**, $r$, is the specified rise of the follower and is constrained to act along the line of motion of the follower.

$$r = c + s(\theta) \tag{5.1}$$

where $c$ is the base circle radius of the cam and $s(\theta)$ is the specified displacement of the follower. Let **l** be the vector, of magnitude $l$, from the tip of vector **r** to the point of contact, **p**. It represents the overhung length of the follower contact (sometimes referred

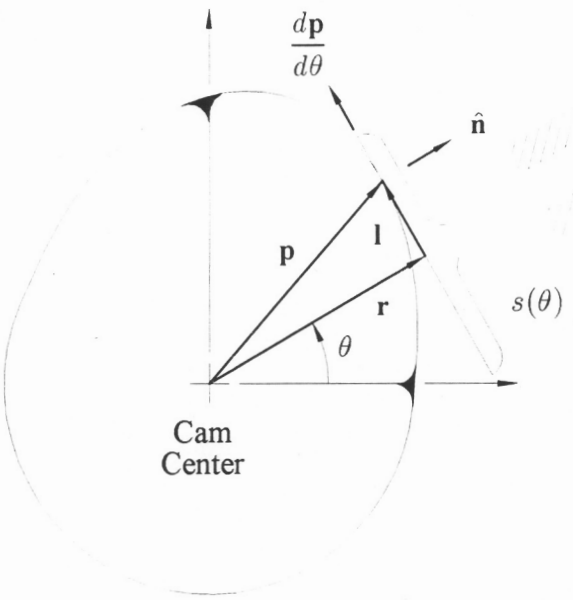


Figure 5.2: Disk Cam With Translating Flat-faced Follower

to as the eccentricity).

The vector **p** locating the point of contact between the cam and follower can be expressed through the follower as

$$\mathbf{p} = \mathbf{r} + \mathbf{l} = re^{i\theta} + le^{i\left(\theta+\frac{\pi}{2}\right)} \tag{5.2}$$

The length $l$ is the only unknown parameter in the vector expression.

Differentiating this equation with respect to $\theta$ produces an expression for the relative velocity between the cam and follower at the point of contact.

$$\frac{d\mathbf{p}}{d\theta} = \frac{dr}{d\theta}e^{i\theta} + rie^{i\theta} + \frac{dl}{d\theta}e^{i\left(\theta+\frac{\pi}{2}\right)} + ile^{i\left(\theta+\frac{\pi}{2}\right)} = \frac{dr}{d\theta}e^{i\theta} + re^{i\left(\theta+\frac{\pi}{2}\right)} + \frac{dl}{d\theta}e^{i\left(\theta+\frac{\pi}{2}\right)} - le^{i\theta} \tag{5.3}$$

Let $\hat{\mathbf{n}}$ be the unit vector along the common normal at the point of contact between the cam and follower. For flat-faced followers, this vector is always perpendicular to the follower face.

$$\hat{\mathbf{n}} = e^{i\theta} \tag{5.4}$$

Because all relative motion must be tangent to both surfaces, the dot product between the relative velocity and the common normal must equal zero. The dot product, also called inner product or scalar product, is defined as the product of the magnitudes of the vectors and the cosine of the angle between them.

$$\hat{\mathbf{n}} \cdot \frac{d\mathbf{p}}{d\theta} = 0$$

$$e^{i\theta} \cdot \left( \frac{dr}{d\theta} e^{i\theta} + r e^{i(\theta+\frac{\pi}{2})} + \frac{dl}{d\theta} i e^{i\theta} - l e^{i\theta} \right) = 0 \tag{5.5}$$

Since $e^{i\theta} \cdot e^{i\theta} = 1$ and $e^{i\theta} \cdot e^{i(\theta+\frac{\pi}{2})} = 0$, the above result simplifies to

$$\frac{dr}{d\theta} - l = 0 \tag{5.6}$$

Differentiating equation 5.1 yields

$$\frac{dr}{d\theta} = \frac{ds}{d\theta} \tag{5.7}$$

This is simply the specified velocity of the follower from the motion program. The motion program is the desired displacement schedule of the follower.

The resulting expression for the cam profile is:

$$\begin{aligned} \mathbf{p} &= r e^{i\theta} + \frac{dr}{d\theta} i e^{i\theta} \\ \mathbf{p} &= (s(\theta) + c)\, e^{i\theta} + \frac{ds}{d\theta} e^{i(\theta+\frac{\pi}{2})} \end{aligned} \tag{5.8}$$

The vector expression in equation 5.8 provides the cam profile for a specified follower motion program, $s(\theta)$, as a function of the cam rotation, $\theta$. Note that the sign of this angle must be changed going from the motion program to equation 5.8. This is a well-known result, but it helps to demonstrate the utility of the conjugate geometry method. The conjugate geometry approach is also useful in designing cams for cam-modulated linkages where the followers often undergo complex motion. It will be used here to formulate the synthesis of wrapping cams.

## 5.4 GGRR Mechanism

The GGRR mechanism has already been introduced. The surface of the cam can be generated to produce a specified position or force response. The distance between the cam and pulley centers, the pulley radius and the thickness of the belt must be given prior to synthesis.

### 5.4.1 Loop Closure and Conjugate Geometry

To generate the cam surface, several design parameters must be defined. As shown in Fig. 5.3, the distance between cam and pulley centers, the pulley radius, and the thickness of the belt are labeled $c$, $r$, and $t$, respectively. The desired function or mechanical

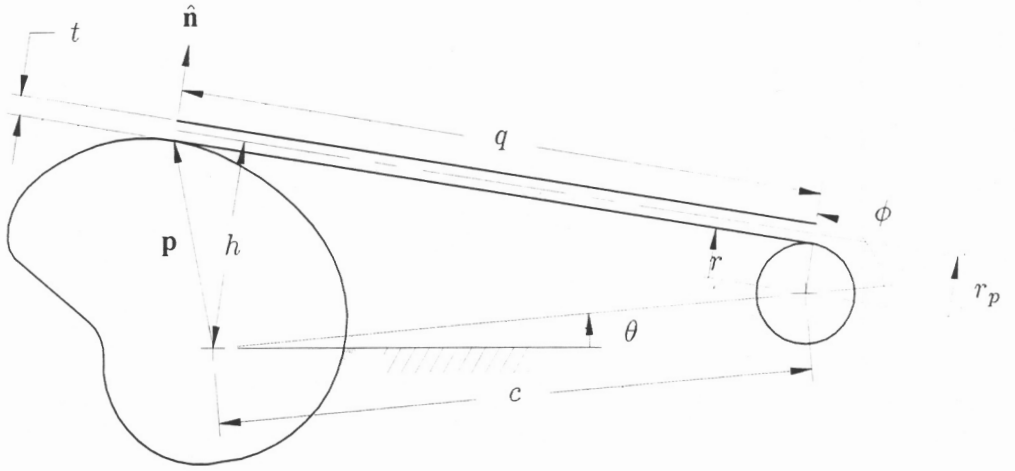


Figure 5.3: GGRR Mechanism, Uncrossed Configuration

advantage relationship must also be given. Let the scalar $r_p$ be defined as the pulley pitch radius, the distance from the pulley center to the center of the belt.

$$r_p = r + \frac{t}{2} \tag{5.9}$$

This variable will simplify the derivation for the crossed configuration. This dimension is also the radius of a sprocket used with roller chains as found in equation 4.21.

The following derivation is based on this inversion where the cam is fixed and all vectors are referenced to a coordinate system attached to the cam. Assuming a taut belt, the line of connection (centerline of the belt) must, by definition, be tangent to the pitch surface of the cam. The vector **p** locates the point on the cam surface where the side of the belt first makes contact. In the inverted mechanism, the angle $\theta$ is the rotation of the pulley center around the cam. If the cam is to rotate in the positive direction, then the pulley will rotate counter-clockwise in the inverted mechanism. Clearly, the tip of vector **p** must travel along the surface of the cam. The vector **p** is expressed in complex polar form in the coordinate system fixed to the cam by traversing a loop through the pulley and back to the contact point.

$$\begin{aligned} \mathbf{p} &= ce^{i\theta} + r_p e^{i(\theta+\phi)} + qe^{i\left(\theta+\phi+\frac{\pi}{2}\right)} + \frac{t}{2}e^{i(\theta+\phi+\pi)} \\ &= ce^{i\theta} + \left(r_p - \frac{t}{2}\right)e^{i(\theta+\phi)} + qe^{i\left(\theta+\phi+\frac{\pi}{2}\right)} \end{aligned} \tag{5.10}$$

In this equation, $q$ is the distance along the line of connection (down the middle of the belt) from the point of contact with the pulley to the point of contact on the cam surface.

At any time, the vector $\frac{d\mathbf{p}}{d\theta}$ must be along the line tangent to the cam surface (on the

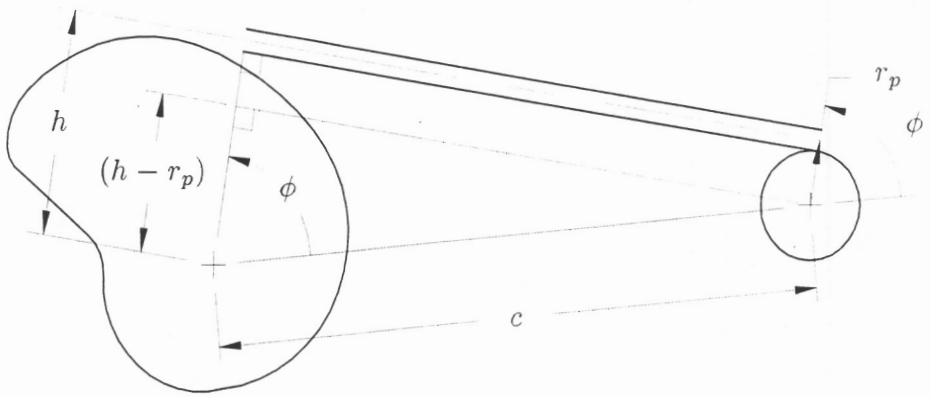


Figure 5.4: Belt Moment Arm in Uncrossed GGRR Mechanism

line of connection). Let the unit vector normal to the surface be $\hat{\mathbf{n}}$. Since the tangent and normal vectors must be orthogonal to each other,

$$\frac{d\mathbf{p}}{d\theta} \cdot \hat{\mathbf{n}} = 0 \tag{5.11}$$

This is the condition of contact for the two conjugate surfaces. It states that the relative direction of the velocity of the point of contact is perpendicular to the normal to the surface [Chakraborty and Dhande, 1977].

The unit vector normal to the surface is

$$\hat{\mathbf{n}} = e^{i(\theta-\phi)} \tag{5.12}$$

where $\phi$ is the angle locating the point of contact between the belt and pulley measured from an extension to the centerline. It is also the angle between the belt moment arm and the centerline.

Differentiating equation 5.10 with respect to the inverted mechanism rotation angle, $\theta$,

$$\begin{aligned} \frac{d\mathbf{p}}{d\theta} &= ice^{i\theta} + i\left(1 + \frac{d\phi}{d\theta}\right)\left(r_p - \frac{t}{2}\right)e^{i(\theta+\phi)} + \frac{dq}{d\theta}e^{i\left(\theta+\phi+\frac{\pi}{2}\right)} + i\left(1 + \frac{d\phi}{d\theta}\right)qe^{i\left(\theta+\phi+\frac{\pi}{2}\right)} \\ &= ce^{i\left(\theta+\frac{\pi}{2}\right)} + \left[\left(1 + \tfrac{d\phi}{d\theta}\right)\left(r_p - \tfrac{t}{2}\right) + \tfrac{dq}{d\theta}\right]e^{i\left(\theta+\phi+\frac{\pi}{2}\right)} + q\left(1 + \tfrac{d\phi}{d\theta}\right)e^{i(\theta+\phi+\pi)} \end{aligned} \tag{5.13}$$

The condition of contact given in equation 5.11 becomes

$$\frac{d\mathbf{p}}{d\theta} \cdot \hat{n} = 0 = c\cos\left(\phi - \frac{\pi}{2}\right) + q\left(1 - \frac{d\phi}{d\theta}\right)\cos(\pi) \tag{5.14}$$

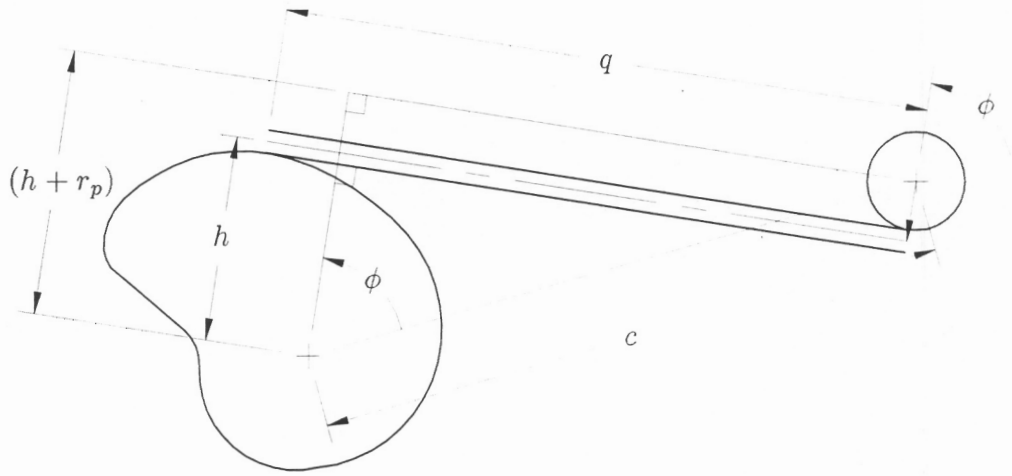


Figure 5.5: GGRR Mechanism, Crossed Assembly

Solving for $q$,

$$q = \frac{c\sin(\phi)}{\left(1 + \frac{d\phi}{d\theta}\right)} \tag{5.15}$$

As shown in Fig. 5.4, $\phi$ can be found from the geometry of the mechanism

$$\cos(\phi) = \frac{(h - r_p)}{c} \tag{5.16}$$

$$\frac{d\phi}{d\theta} = \frac{-1}{\sqrt{c^2 - (h - r_p)^2}} \left(\frac{dh}{d\theta}\right) \tag{5.17}$$

### 5.4.2 Crossed Assembly

If the belt crosses the centerline between the cam and pulley, a different closure or branch of the mechanism results. The synthesis differs only slightly from the uncrossed case. The direction of motion is changed. The vector expressing the location of the contact point **p** becomes

$$\mathbf{p} = ce^{i\theta} + \left(\frac{t}{2} - r_p\right) e^{i(\theta+\phi)} + qe^{i\left(\theta+\phi+\frac{\pi}{2}\right)} \tag{5.18}$$

Equation 5.15 for $q$ remains the same because the $\left(\frac{t}{2} - r_p\right)$ term drops out. As shown in Fig. 5.5, $\phi$ can be found from the geometry of the mechanism

$$\cos(\phi) = \frac{(h + r_p)}{c} \tag{5.19}$$

Therefore,

$$\frac{d\phi}{d\theta} = \frac{-1}{\sqrt{c^2 - (h + r_p)^2}} \left(\frac{dh}{d\theta}\right) \tag{5.20}$$

### 5.4.3 Force Synthesis

The GGRR mechanism can be used to generate a specified mechanical advantage relationship. This can be specified as a desired torque in the pulley and cam. The designer must decide which element (the cam or the pulley) is the input and which is the output. In many cases, the cam can be either; see Section 3.5. The relative direction of the desired torques will dictate whether the the crossed or uncrossed configuration is needed.

Let the torque exerted on the cam and pulley be $T_c$ and $T_p$, respectively. If the torques act in the opposite directions, the crossed configuration must be used; otherwise the uncrossed mechanism is needed. Let the torque applied to the cam be defined over the range $\theta \in [0, \theta_{\max}]$ as $T_c(\theta)$. This produces a torque in the pulley, $T_p(\psi)$. where $\psi \in [0, \psi_{\max}]$. These torques are not arbitrary because work must be conserved between the cam and pulley

$$\int_0^{\theta} T_c \, d\theta = \int_0^{\psi} T_p \, d\psi \tag{5.21}$$

Typically, the output torque function is defined as a function of its rotation over a given range. The input torque is known as a function of its rotation. The relationship between input and output rotations and the range of motion of the input can be found by integrating equation 5.21, if possible.

Equation 5.21 can also be solved as a differential equation of the mechanical advantage relationship of the device.

$$\frac{d\psi}{d\theta} = \frac{T_c}{T_p} \tag{5.22}$$

Let $F$ be defined as the tension in the belt. At any position $\theta$ and corresponding position $\psi$,

$$T_p(\theta) = r_p F \qquad \text{and} \qquad T_c(\psi) = hF \tag{5.23}$$

Eliminating $F$ from these two equations yields

$$\frac{T_p}{r_p} = \frac{T_c}{h} \tag{5.24}$$

which can be solved for $h$.

$$h = r_p \frac{T_c}{T_p} \tag{5.25}$$

The torque in the pulley cannot be zero because this would require an infinite moment arm, $h$.

Differentiating with respect to the cam rotation angle,

$$\frac{dh}{d\theta} = r_p \frac{T_p \frac{dT_c}{d\theta} - T_c \frac{dT_p}{d\theta}}{(T_p)^2} \tag{5.26}$$

where

$$\frac{dT_p}{d\theta} = \frac{dT_p}{d\psi}\frac{d\psi}{d\theta}$$

Given the mechanical advantage requirements along with the belt thickness, center distance, and pulley radius, the surface of the cam can be found. The range of input angles is divided into a number of increments. At each, the resulting point of contact on the surface of the cam is calculated.

$$\mathbf{p} = ce^{i\theta} + \left(\pm r_p - \frac{t}{2}\right) e^{i(\theta+\phi)} + \frac{c\sin(\phi)}{\left(1+\frac{d\phi}{d\theta}\right)} e^{i\left(\theta+\phi+\frac{\pi}{2}\right)} \tag{5.27}$$

where the sign of $r_p$ depends on the relative direction of the desired torques. This process results in a number of points defining the surface of the cam. The set of these points over the range $\theta \in [0, \theta_{\max}]$ defines the surface of the cam.

### 5.4.4 Function Generation

The GGRR mechanism can also be used to accurately produce a given position function of an input rotation. A relationship is desired between $\psi$ and $\theta$, either

$$\psi = f(\theta) \qquad \text{or} \qquad \theta = g(\psi) \tag{5.28}$$

The belt velocity at cam surface must be equal to the belt velocity on the surface of the pulley.

$$h\frac{d\theta}{dt} = r_p \frac{d\psi}{dt} \tag{5.29}$$

Therefore

$$h = r_p \frac{d\psi}{d\theta} \tag{5.30}$$

where

$$\frac{d\psi}{d\theta} = \frac{df}{d\theta} \qquad \text{or} \qquad \frac{d\psi}{d\theta} = \left(\frac{dg}{d\psi}\right)^{-1} = \frac{d\psi}{dg}$$

and

$$\frac{dh}{d\theta} = r_p \frac{d^2\psi}{d\theta^2} \tag{5.31}$$

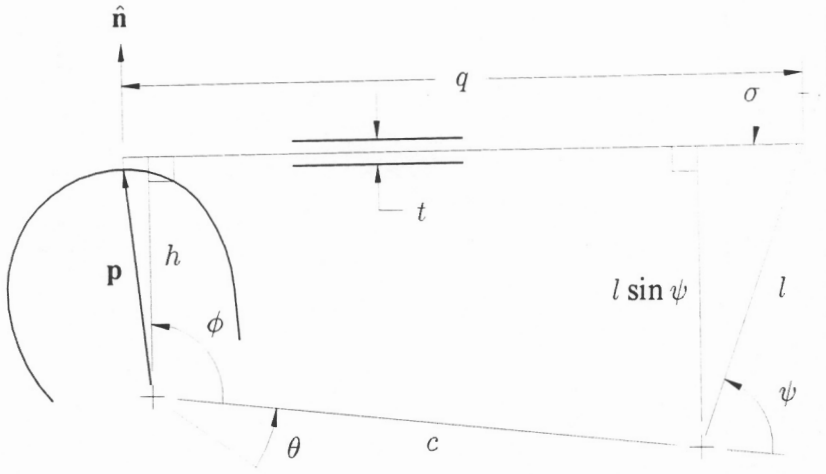


Figure 5.6: GRRR Mechanism

where

$$\frac{d^2\psi}{d\theta^2} = \frac{d^2 f}{d\theta^2} \qquad \text{or} \qquad \frac{d^2\psi}{d\theta^2} = \frac{d^2\psi}{dg^2}$$

These two results can be substituted into either equations 5.16 and 5.17 or equations 5.19 and 5.20 to find $\phi$ and its derivative with respect to $\theta$. Therefore, $q$ and the surface of the cam **p** can be found. This can be done for either the crossed or uncrossed configurations.

## 5.5 GRRR Mechanism

The GRRR mechanism was discussed in Chapters 3 and 4. This mechanism can be used to produce a specified position or force response. The center distance between the cam and link pivot, $c$,, the link length from the pivot to the belt connection, $l$, and the thickness of the belt, $t$, must be given prior to the beginning of synthesis.

### 5.5.1 Loop Closure and Conjugate Geometry

As shown in Fig. 5.6, let $l$ be the length of the link from the pivot to the belt connection, $c$ be the distance between the cam center and link pivot, and $q$ be the variable representing the free length of belt between the point of contact on the cam and the connection to the link.

The vector loop expression of the location of the point of contact is

$$\mathbf{p} = ce^{i\theta} + le^{i(\theta+\psi)} + qe^{i(\theta+\psi+\sigma)} + \frac{t}{2}e^{i\left(\theta+\psi+\sigma+\frac{\pi}{2}\right)} \tag{5.32}$$

Differentiating the equation for the cam contact point with respect to the cam rotation.

$$\begin{aligned}\frac{d\mathbf{P}}{d\theta} &= ice^{i\theta} + i\left(1+\tfrac{d\psi}{d\theta}\right)e^{i(\theta+\psi)} + \tfrac{dq}{d\theta}e^{i(\theta+\psi+\sigma)} \\ &\quad +i\left(1+\tfrac{d\psi}{d\theta}+\tfrac{d\sigma}{d\theta}\right)qe^{i(\theta+\psi+\sigma)} + i\left(1+\tfrac{d\psi}{d\theta}+\tfrac{d\sigma}{d\theta}\right)\tfrac{t}{2}e^{i\left(\theta+\psi+\sigma+\frac{\pi}{2}\right)}\end{aligned}$$

$$= ce^{i\left(\theta+\frac{\pi}{2}\right)} + \left(1+\tfrac{d\psi}{d\theta}\right)e^{i\left(\theta+\psi+\frac{\pi}{2}\right)} + \left(\tfrac{dq}{d\theta}-\tfrac{t}{2}\right)e^{i(\theta+\psi+\sigma)} + q\left(1+\tfrac{d\psi}{d\theta}+\tfrac{d\sigma}{d\theta}\right)e^{i\left(\theta+\psi+\sigma+\frac{\pi}{2}\right)} \tag{5.33}$$

The unit vector normal to the surface of the cam is

$$\hat{\mathbf{n}} = e^{i\left(\theta+\psi+\sigma-\frac{\pi}{2}\right)} \tag{5.34}$$

The condition of contact for the two conjugate surfaces implies that velocity of the point of contact is perpendicular to the normal to the surface [Chakraborty and Dhande, 1977]. Thus,

$$\frac{d\mathbf{P}}{d\theta}\cdot\hat{\mathbf{n}} = 0 = c\cos(\psi+\sigma-\pi)+\left(1+\frac{d\psi}{d\theta}\right)\cos(\sigma-\pi)+q\left(1+\frac{d\psi}{d\theta}+\frac{d\sigma}{d\theta}\right)\cos(-\pi) \tag{5.35}$$

Solving for $q$,

$$q = \frac{-c\cos(\psi+\sigma)-\left(1+\frac{d\psi}{d\theta}\right)\cos\sigma}{\left(1+\frac{d\psi}{d\theta}+\frac{d\sigma}{d\theta}\right)} \tag{5.36}$$

The angle, $\phi$, between the centerline, $c$, and belt moment arm, $h$, can be found from the geometry of the mechanism.

$$\phi = \cos^{-1}\left(\frac{h-l\sin\psi}{c}\right) \tag{5.37}$$

for the uncrossed configuration shown in Fig. 5.6.

This gives the angle between the link and belt $\sigma$ directly.

$$\sigma = \phi - \psi + \frac{\pi}{2} \tag{5.38}$$

Differentiating the above equation gives

$$\frac{d\sigma}{d\theta} = \frac{d\phi}{d\theta} - \frac{d\psi}{d\theta} \tag{5.39}$$

where

$$\frac{d\phi}{d\theta} = \frac{\left(l\cos\psi\frac{d\psi}{d\theta}-\frac{dh}{d\theta}\right)}{\sqrt{c^2-(h-l\sin\psi)^2}} \tag{5.40}$$

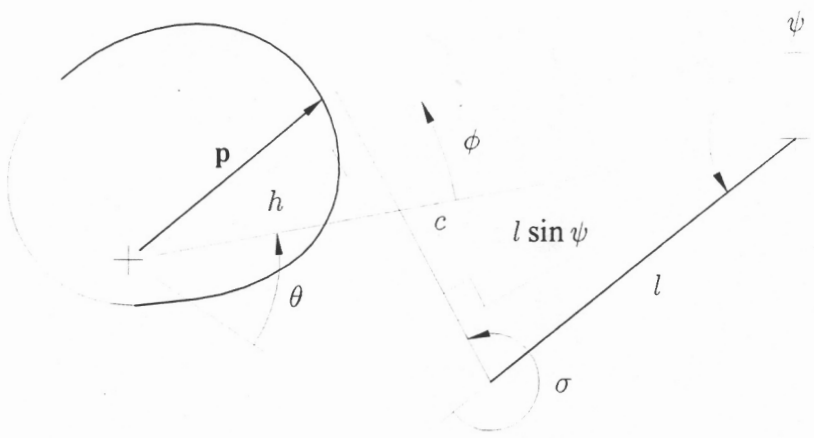


Figure 5.7: GRRR Mechanism, Crossed Configuration

### 5.5.2 Crossed Assembly

The crossed assembly of the GRRR mechanism occurs when the belt crosses the centerline between the cam and link. The rotation of the link and cam are opposite in direction. The same vector loop equation as in the uncrossed GRRR assembly (equation 5.32) is used.

The angle between the belt moment arm and the centerline can also be found from the geometry of the mechanism.

$$\phi = \cos^{-1}\left(\frac{h + l\sin\psi}{c}\right) \tag{5.41}$$

Differentiating

$$\frac{d\phi}{d\theta} = \frac{\left(-\frac{dh}{d\theta} - l\cos\psi\frac{d\psi}{d\theta}\right)}{\sqrt{c^2 - (h + l\sin\psi)^2}} \tag{5.42}$$

The equations for $\sigma$ and its derivative are the same as for the uncrossed case. Equation 5.32 can therefore be used to generate the surface of the cam for function generation.

### 5.5.3 Force Synthesis

The GRRR mechanism can be used to generate force relationships as well by specifying a torque on both the cam and link. The relative direction of the these torques will dictate whether the crossed or uncrossed configuration is needed. The designer must choose which element is the input and which is the output. In many cases, the cam can be either (see Section 3.5).

Let the torque in the cam be defined over the range $\theta \in [0, \theta_{\max}]$ as $T_c(\theta)$. This produces a torque in the link, $T_l(\psi)$ where $\psi \in [\psi_{\min}, \psi_{\max}]$. The starting angle of the

link, $\psi_{\min}$, must be given. The torques are not arbitrary because conservation of work must be conserved between the cam and link

$$\int_0^{\theta} T_c \, d\theta = \int_{\psi_{\min}}^{\psi} T_l \, d\psi \tag{5.43}$$

If the output torque function is defined as a function of its rotation over a given range and the input torque is known as a function of its rotation, then the relationship between input and output rotations and the range of motion of the input can be found from equation 5.43.

Equation 5.43 can also be written as a differential equation.

$$\frac{d\psi}{d\theta} = \frac{T_c}{T_p} \tag{5.44}$$

Let $F$ be defined as the tension in the belt. At any position $\theta$ and corresponding position $\psi$,

$$T_l(\theta) = l \sin\psi F \qquad \text{and} \qquad T_c(\psi) = hF \tag{5.45}$$

Eliminating $F$ and solving these two equations yields

$$\frac{T_l}{l \sin\psi} = \frac{T_c}{h} \tag{5.46}$$

or

$$h = \frac{T_c}{T_l} l \sin\psi \tag{5.47}$$

The angle $\phi$ and its derivative can be found from the geometry of the mechanism depending on the assembly of the mechanism (crossed or uncrossed). The scalar $q$ can be calculated and substituted into equation 5.32 to find the point on the surface of the cam. This process is repeated for different values of the cam rotation until the cam surface is determined.

### 5.5.4 Function Generation

The GRRR mechanism can be used to achieve a position as a function of an input rotation. A mathematical relationship is given between $\psi$ and $\theta$ either

$$\psi = f(\theta) \qquad \text{or} \qquad \theta = g(\psi) \tag{5.48}$$

The belt velocity at the cam surface must be equal to the belt velocity at the link connection.

$$h\frac{d\theta}{dt} = l \sin\psi \frac{d\psi}{dt} \tag{5.49}$$

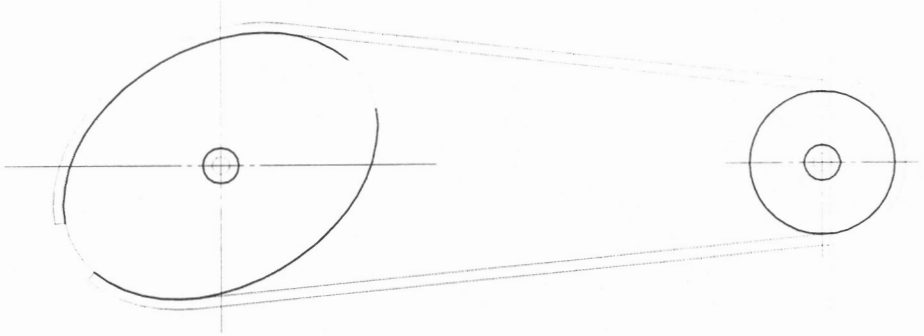

Figure 5.8: Wrapping Cam Mechanism with Two Belts

Therefore

$$h = l \sin\psi \frac{d\psi}{d\theta} \tag{5.50}$$

where

$$\frac{d\psi}{d\theta} = \frac{df}{d\theta} \qquad \text{or} \qquad \frac{d\psi}{d\theta} = \frac{d\psi}{dg} = \left(\frac{dg}{d\psi}\right)^{-1}$$

and

$$\frac{dh}{d\theta} = l\cos\psi \left(\frac{d\psi}{d\theta}\right)^2 + l\sin\psi \frac{d^2\psi}{d\theta^2} \tag{5.51}$$

where

$$\frac{d^2\psi}{d\theta^2} = \frac{d^2f}{d\theta^2} \qquad \text{or} \qquad \frac{d^2\psi}{d\theta^2} = \frac{d^2\psi}{dg^2}$$

Thus, $\phi$ and its derivative can be found. Therefore, $q$ and the surface of the cam $\mathbf{p}$ can be calculated. This can be done for both the crossed or uncrossed configurations.

## 5.6 Conclusions

Synthesis methods have been presented for the GGRR and GRRR mechanisms. These mechanisms were chosen as examples because they appear to be the most practical and the most commonly used. The same methods can be used to develop synthesis algorithms for the other wrapping cam mechanisms enumerated in Chapter 3.

In reciprocating systems, the cam profile must be generally less than 360 degrees or the belt must move out of its original plane of motion. The designer must finish the profile to allow for belt connection without causing interference with other parts of motion. In continuous belt systems, rotation is typically in one direction. The design curves are

therefore limited because they must generate a closed surface for the cam. Otherwise, the same methods can be used for synthesis.

In some applications of function generation, it is desirable to use two belts and generate two cam profiles to insure that the mechanism can be driven in both directions as shown in Fig. 5.8. Such a mechanism would have the advantage of very little backlash. The range of motion is reduced if the mechanism remains planar but not if the two belts are slightly offset out of the plane of motion.

Techniques for synthesis of wrapping cams have been developed. When implemented on a computer, these allow for the quick generation of cam surfaces. This allows cam designs to be quickly produced with very little error.

# Chapter 6

# Applications and Verifications

Wrapping cam mechanisms have many possible applications. Most applications are more complicated than the simple problems of force and function generation presented previously. This opportunity will be used to explore some of these applications and to verify the techniques developed in Chapters 4 and 5.

## 6.1 Application of the GGRR Mechanism to Exercise Equipment

For optimum exercise, the applied force should mirror the user's strength at each point throughout the range of motion in the exercise. When this occurs, the muscle fibers exercised will be fatigued over the entire range of motion promoting strength improvement throughout this range. Good exercise equipment is designed to vary the exercise force to do this. A properly designed GGRR wrapping cam mechanism can be used in an exercise machine to fulfill this need exactly.

The force distributions are obtained from physical testing of a variety of individuals. These curves are normalized and combined into an ideal force curve. For the exercise machine, this translates into a particularly shaped force distribution as a function of the rotation of a mechanical member. This output may be either the cam or pulley. The force magnitude will change depending on the particular user with a user selected input weight. To put as much force on the user as possible with a limited weight, this weight stack should be lifted as far as possible given the constraints of the machine. Let this distance be labeled $L$. The mechanical advantage needed by the mechanism, $t(\theta)$, is a function of the rotation of the output. The designer must choose whether the cam or pulley is this output element.

Because of the high forces and long-term cyclic loading, a roller chain is chosen instead of a belt. For these tests, ANSI type 40 chain was chosen as the particular wrapping follower.

These design requirements maybe transformed into the force generation problem described in Section 5.4.3 given the range of input and output rotation and the shape of the output force requirements. If the chain is attached to the weight stack after passing over the pulley, the cam is the output. This is referred to as the *constant chain tension* problem.

The torque applied to the pulley, $T_p$, is

$$T_p = r_p W \tag{6.1}$$

where $W$ is the weight on the machine. The value $r_p$ is the pitch radius of the pulley defined as the distance between the center of the pulley and the center of the rollers on the chain wrapping it.

The torque to be applied to the cam is

$$T_c = kt(\theta) \tag{6.2}$$

where $k$ is an unknown constant

The work done lifting the weight stack is

$$\int_0^L W dx = LW = \int_0^\theta kt(\theta) d\theta \tag{6.3}$$

which can be solved for the constant $k$

$$k = \frac{LW}{\int_0^\theta t(\theta) d\theta} \tag{6.4}$$

The value for $W$ drops out of these equations. The mechanical advantage relationship of the device is,

$$\frac{T_c}{T_p} = \frac{t(\theta)L}{r_p \int_0^\theta t(\theta) d\theta} \tag{6.5}$$

This result defines the moment arm, $h$, found using equation 5.25.

$$\frac{dh}{d\theta} = \frac{r_p L}{r_w \int_0^\theta t(\theta) d\theta} \frac{dt}{d\theta} \tag{6.6}$$

where $\frac{dt}{d\theta}$ can be found explicitly from the equation of the polynomial $t(\theta)$. The surface of the cam can now be synthesized.

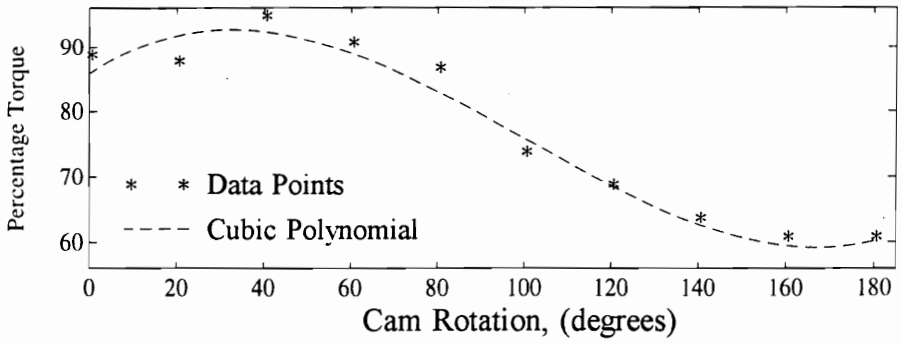


| $\theta$ | $t(\theta)$ |
|---|---|
| 0 | 88 |
| 20 | 87 |
| 40 | 94 |
| 60 | 90 |
| 80 | 86 |
| 100 | 73 |
| 120 | 68 |
| 140 | 63 |
| 160 | 60 |
| 180 | 60 |

Figure 6.1: Mechanical Advantage Relationship for a Typical Exercise Machine

### 6.1.1 Synthesis of a Constant Chain Tension Force Generator

In this example, it is assumed that a discrete set of required torque values has been found experimentally as shown in Fig. 6.1.

In order to produce a smooth torque profile, a cubic curve is fit through the given data using the least-square method as shown by the dashed line in Fig. 6.1 [MathWorks, 1993]. A smooth torque curve has the advantage of producing smooth motion in the resulting mechanism.

Given the distance between the centers of the cam and pulley is 27.9 cm, the pulley radius (with 19 teeth) is 3.86 cm, the movement of the weight stack is 16 cm, and chain thickness (for ANSI type 40) is 1.19 cm, the synthesis process produces the pitch surface and cam profile shown in Fig. 6.2.

### 6.1.2 Analysis of a Constant Chain Tension Force Generator

The cam generated above can now be analyzed using the geometric method described in Section 4.3. A quartic curve is fit to points on the cam shown in Fig. 6.2. The error between the curve and the cam in less than 0.02 cm. The cam torque is calculated, and the result is shown in Fig. 6.3 with the original torque requirements. As this figure shows, the torque calculated from the synthesized cam surface matches the desired torque almost exactly.

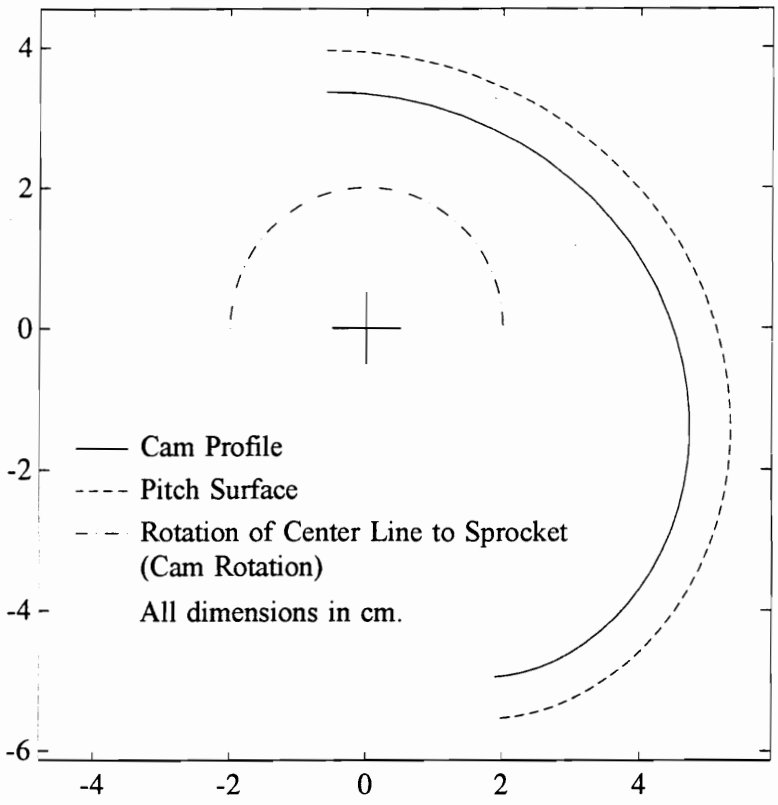

Figure 6.2: Synthesized Cam

### 6.1.3 Discussion

The original and calculated torque curves shown in Fig. 6.3 are very close, but the calculated cam rotation angles do not start at 0 degrees or end at 180°. This is caused by small errors in the derivative of the curve fitted to the cam. It produces large errors in torque curve angles (4 degrees in this case) but good values of torque (a difference of only 0.4). These errors can be mitigated by weighting the points at the ends of the cam surface more heavily when curve fitting.

The same mechanism could be used with a varying input weight instead of a constant. This situation arrises if weight plates are added to the end of a rotating arm instead of plates pinned to a vertically moving stack. The input force would vary with the sine of the orientation of the weighted link. If the range of rotation is specified, this changing weight is integrated when calculating the work in equation 6.3.

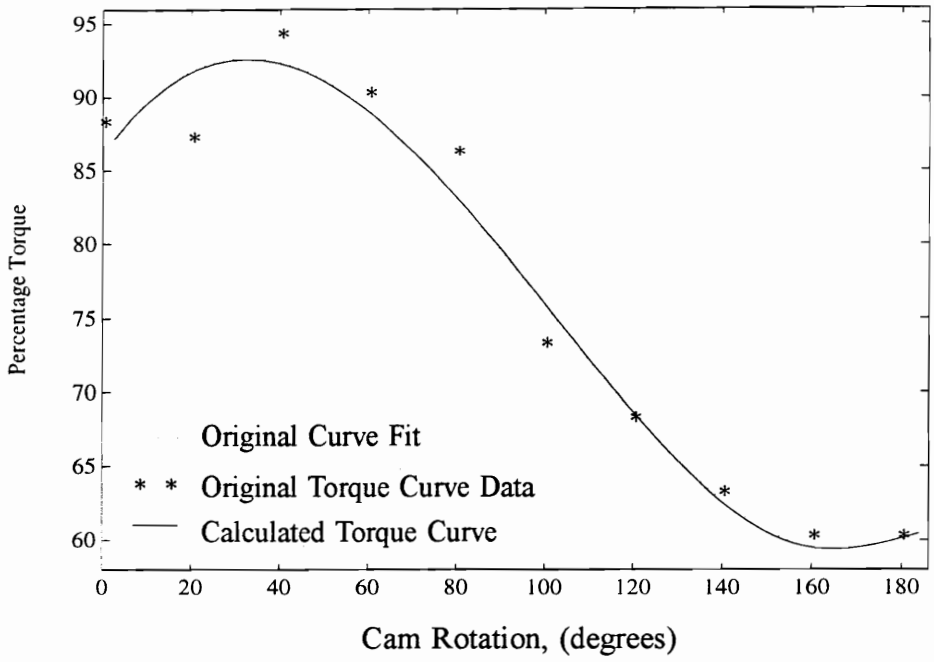


Figure 6.3: Calculated Torque Curve with Original

### 6.1.4 Experimental Test Setup and Data Acquisition Equipment

A testing apparatus and data acquisition system was assembled to experimentally verify the effectiveness of the cam synthesis procedure. The kinematic synthesis and analysis procedures have been shown to be in agreement with each other in the previous sections. Experimental verification gives further credibility to these results and also helps in understanding how unmodeled effects such as friction, dynamics and compliance of the actual machine may contribute to the overall design.

A schematic diagram of the test rig, which was developed jointly with Nautilus, is shown in Fig. 6.4. The equipment was designed to simultaneously sample the rotational position of the output link and the force output for both constant chain tension and constant torque cam and follower arrangements. A potentiometer is used to directly measure the angular position of the output link, which is connected to a circular output sprocket. A load cell is attached to directly acquire the magnitude of the ouput force. The load cell was connected to a PC-based data acquisition system via a strain indicator, which functioned to process and condition the output signal of the load cell. The load cell signal and the potentiometer voltage were then sampled by an analog-to-digital converter and then processed in a custom-written computer program. The program output is a plot of

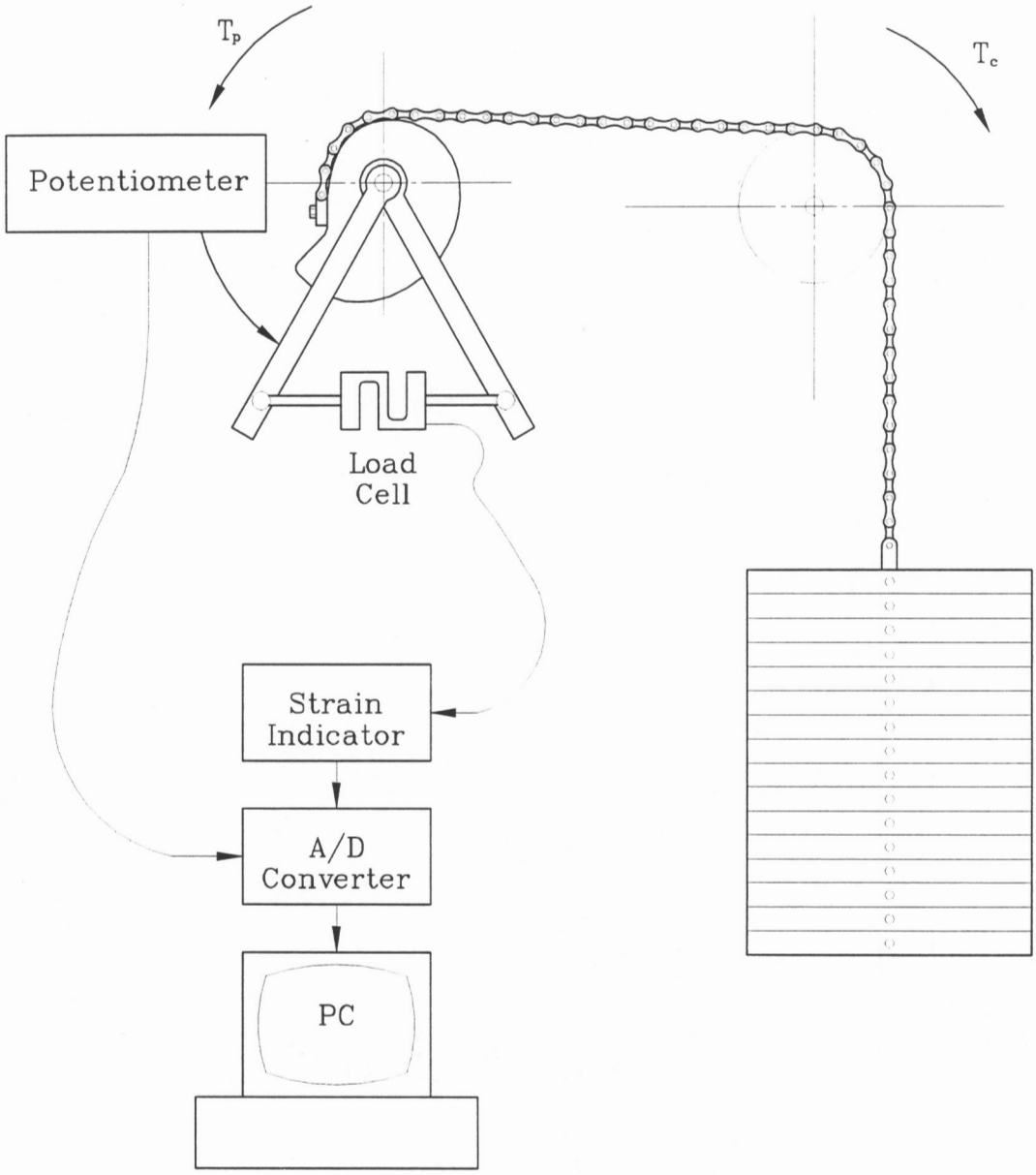


Figure 6.4: Schematic Diagram of the Experimental Test Rig

the force curve of the cam being used in the test-rig.

Initial force data produced by the test was far more erratic than expected, although the general trends of the curves were believed to be correct. Much of the noise was determined to be low level electrical noise and the effects of dynamic loading of the test-rig during data acquisition. The removal of the dynamic loading problem was more complicated. The test-rig was adapted by adding a worm-gear drive system. This system allows the output to be incremented from point to point, so that all measurements are static. While this does produce better data for kinematic synthesis verification, it is also an indication of a potential problem in real equipment. In the future, it may be necessary to consider dynamic effects as part of the synthesis process, although this is beyond the scope of the present work. The effects of noise were further reduced by taking 1000 data points at one incremental position and averaging the results. This averaging was done for both angular and force data.

The load cell and the potentiometer were calibrated so that the load cell and the angular voltages could be converted to a scalar weight and angle measurements respectively. These calibration factors were included in the data acquisition software as constants which convert the voltage signal of either the force or the angle to either pounds or degrees by simple multiplication. Force curves could then be acquired with this modified data acquisition system.

Force curves for both the constant chain tension and constant torque cam and configurations were taken using the test rig and data acquisition equipment. Several important general observations can be made about the resulting data. The equipment produces force curves which have a high degree of repeatability. The incremental points where the chain links contact the cam surface (the chordal effect) is frequently evident in the force curve. The force curve produced when lowering the weight is consistently lower than the force curve produced when raising the weight by about three pounds. This hysteresis is an excellent example of how sensitive the data acquisition equipment is to the friction in the test rig.

### 6.1.5 Analysis of a Constant Chain Tension Force Generator

The test rig was configured as shown in Fig. 6.4 with a weight stack hug from the sprocket with a chain. The chain then wrapped the cam. The force curves produced by the test rig in this configuration have been used to verify the cam synthesis software. Force measurements were taken as the was mechanism moved through it range. Force curve

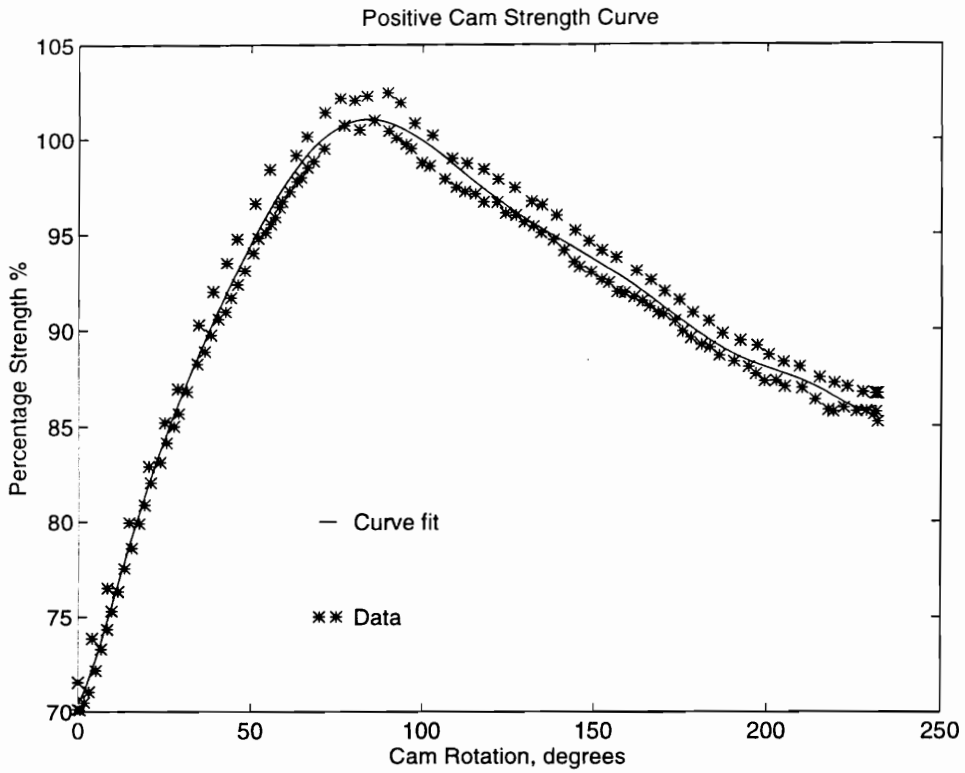


Figure 6.5: Experimental Force Data

data is read directly into the synthesis software and a cam surface is generated. This cam surface can be compared to the actual cam in the test-rig which generated the original force curve.

Force data for the constant torque cam is shown in Fig. 6.5. A polynomial was fit to the data using the method of least-squares. The effects of friction yield the two sets of points on the graph.

The calculated polynomial with the other dimensions from the test rig were used to calculate a theoretical cam surface. The calculated and original cam surfaces are shown in Fig. 6.6. The errors are due to cam surface and force measurement errors.

This further demonstates the validity of the synthesis method.

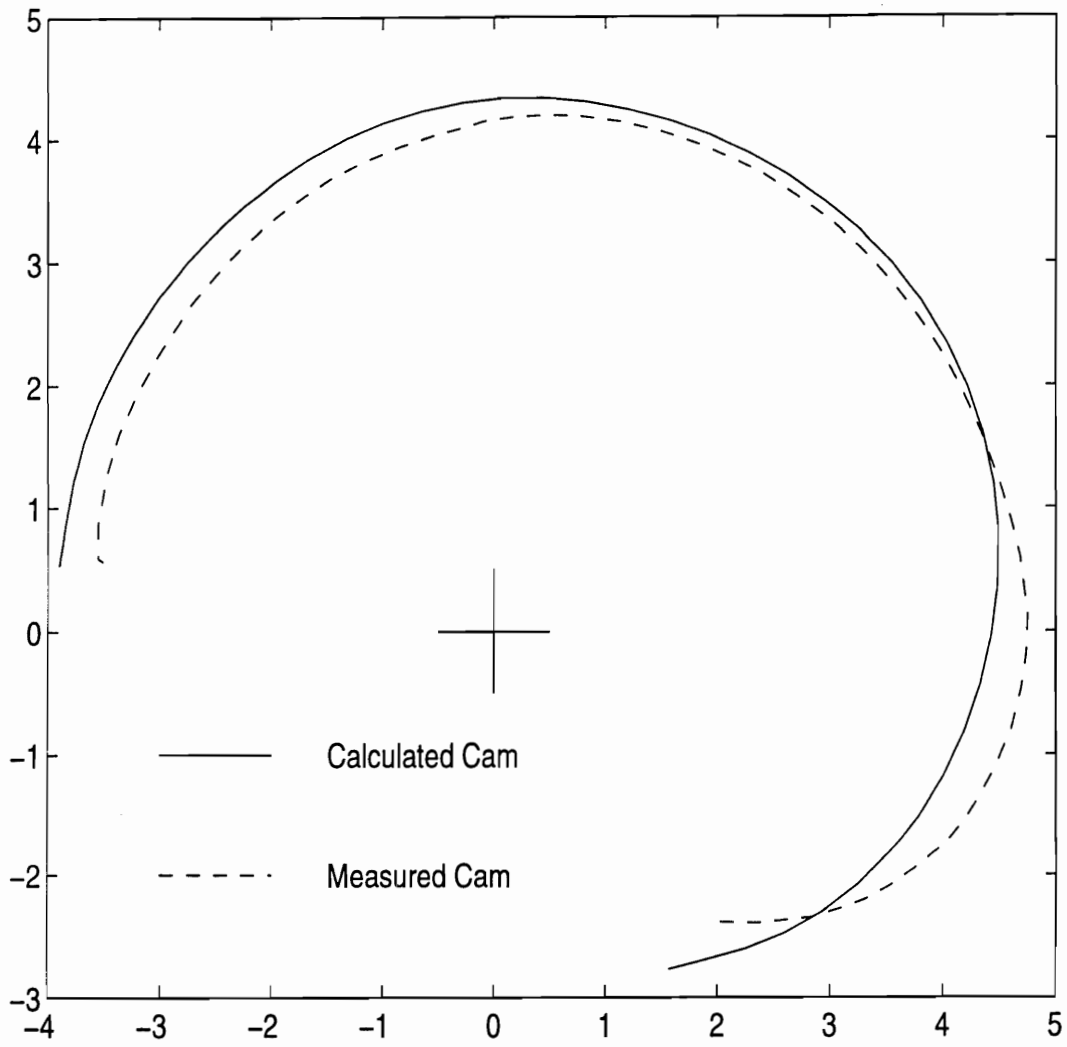


Figure 6.6: Cam Synthesized from Experimental Force Data

# Chapter 7

# Conclusions

## 7.1 Conclusions

This dissertation has presented novel methods for the enumeration, analysis, and synthesis of wrapping cam mechanisms. As part of the enumeration process, two forms of wrapping cam mechanisms believed to be of particular importance were studied in detail. Kinematic analysis techniques were developed to determine the relative positions and internal static forces in the mechanism. Extensive closed-form synthesis techniques have also been developed. While wrapping cam mechanisms have been used for many years in applications such as exercise equipment and counter-balancing devices, methods for analytical analysis and synthesis have not previously been available. This dissertation will join a large body of literature on cam mechanisms. The goal achieved by this work are tools that engineers can use to design wrapping cam mechanisms.

## 7.2 Further Work

This dissertation has presented the first comprehensive kinematic study of basic wrapping cam mechanisms. Nevertheless, many significant areas of related research remain open for studying.

For example, the effect of using a roller chain as a follower should be studied in greater detail. The chain only contacts the cam at discrete locations. This chordal effect has been observed experimentally and could be incorporated into the design process. Design tools could also be developed to synthesize toothed cams (noncircular sprocket) instead of a smooth cams. Although these are more difficult to manufacture, this has the advantage of loading the chain on the rollers instead of on the side plates of the roller chain.

Dynamic effects should be incorporated into the synthesis and analysis procedures for mechanisms operating at high velocities and accelerations.

In automotive applications, performance can be greatly enhanced by modifying the valve timing. The cam follower mechanism can be changed in small ways. Similar advantages may be achieved with wrapping cam mechanisms. Adaptive mechanisms where link lengths and even the surface of the cam may be changed to improve operation should be addressed.

Extensive force synthesis methods have been developed for wrapping cam mechanisms, but more work should be done to develop methods for force synthesis for other mechanisms. The four-bar mechanism is an ideal choice. It can be used in many of the same applications as wrapping cam mechanisms and can be designed to operate with little friction.

# References


1. Binder, R.C., 1956, **Mechanics of the Roller Chain Drive,** Prentice-Hall, Englewood Cliffs, N.J., pp. 75-99.
2. Browning, 1995, *Archery 1995,* sales brochure.
3. Ananthasuresh, G.K. and S. Kota, 1993, "Historical Review of Type Synthesis and Creatic Design," *Modern Kinematics,* A.G. Erdman ed., John Wiley & Sons, New York, pp. 30-36.
4. Bokelberg, E.H. and B.J. Gilmore, 1990, "A Kinematic Design Methodology for Exercise/Rehabilitation Machines Using Springs and Mechanical Advantage to Provide Variable Resistance," *Flexible Mechanism, Dynamics, and Robot Trajectories,* Proceedings 21st Biennial Mechanisms Conference, ASME, New York, pp. 279-286.
5. Chakraborty, J. and S.G. Dhande, 1977, **Kinematics and Geometry of Planar and Spatial Cam Mechanisms,** J. Wiley & Sons, New York,.
6. Chironis, N.P., ed., 1965, **Mechanisms, Linkages, and Mechanical Controls,** McGraw-Hill, New York, pp. 241-245.
7. Chironis, N.P., ed., 1965, **Mechanisms, Linkages, and Mechanical Controls,** McGraw-Hill, New York, pp. 241-245.
8. Chironis, N.P., 1965, **Mechanisms, Linkages, and Mechanical Controls,** McGraw-Hill, New York, p. 136.
9. Chironis, N.P., 1991, **Mechanisms, and Mechanical Devices Sourcebook,** McGraw-Hill, New York, p. 152.
10. Csatari, J., 1994, "Worth the Weight," *Men's Health,* December, pp. 76-78.
11. Eventoff, A.T., 1992, "Automated Cam-Mechanism Synthesis and Analysis," *Mechanism Design and Synthesis - Proceedings of the 1992 ASME Design Technical Conferences*, DE-Vol. 46, pp. 211-224.
12. Freudenstein, F. and C. Chen, 1991, "Variable-Ratio Chain Drives with Noncircular Sprockets and Minimum Slack – Theory and Application," *ASME, Journal of Mechanical Design,* Vol. 113, September, pp. 253-262.
13. Fry, M., 1945, a, "Designing Computing Mechanisms, Part II—Multipying and Dividing," *Machine Deisgn,* Vol. 17, #9, September, pp. 113-120.
14. Fry, M., 1945, b, "Designing Computing Mechanisms, Part III—Cam Mechanisms," *Machine Deisgn,* Vol. 17, #10, October, pp. 123-128.
15. Goodman, T.P., 1965, "Toggle Linkage Applications in Different Mechanisms," , *Mechanisms, Linkages, and Mechanical Controls,* Chironis, N.P., ed., McGraw-Hill, New York, pp. 154-155.

16. Hain, K., 1970, "Challenge: To Design Better Cams," *Journal of Mechanisms,* ed. F.R.E. Crossley Vol.5, #3, Autumn, pp. 283-286.

17. Hain, K., 1967, **Appied Kinematics,** ed. D.P. Adams, McGraw-Hill, New York, pp. 40-42.

18. Hall, A.S., 1961, **Kinematics and Linkage Design,** Prentice-Hall, Englewood Cliffs, N.J., pp. 4, 47.

19. Harmening, W.A., 1974, "Static Mass Balancing with a Torsion Spring and Four-Bar Linkage," ASME, 74-DET-29.

20. Harrison, J.Y., 1970, "Maximizing Human Power Output by Suitable Selection of Motion Cycle Load," *Human Factors,* Vol. 12, No. 3, pp. 315-329.

21. Hartenburg., R.S. and J. Denavit, 1964, **Kinematic Synthesis of linkages,** McGraw-Hill, New York, pp. 222-224 and 242-244.

22. Huang C. and B. Roth, 1994, "Position-Force Synthesis of Closed-Loop Linkages," *ASME, Journal of Mechanical Design,* Vol. 116, March, pp. 155-162.

23. Huey, C.O. and M.W. Dixon, 1974, "The Cam-Link Mechanism for Structural Error-Free Path and Function Generation," *Mechanism and Machine Theory*, Pergamon Press, Vol. 9, pp. 367-374.

24. Jo, D.Y. and Haug, E.J., 1982, "Optimization of Force Balancing Mechanisms," *U.S. Army Tank-Automotive Command Research and Development Center,* Warren, MI., Technical Report No. 12643, March.

25. Kloomok M. and R.V. Muffley, 1955, "Plate Cam Design—with Emphasis on Dynamic Effects," *Product Engineering,* February. Vol. 26 # 2 pp. 156-162.

26. Kloomok M. and R.V. Muffley, 1957, "Computers Simplify Solutions of Polynomial Cam Curves," *Product Engineering,* March. Vol. 28 # 3 pp. 196-202.

27. Kochev, I.S., 1990, "General Method for Active Balancing of Combined Shaking Moment and Torque Fluctuations in Planar Linkages," *Journal of Mechanisms and Machine Theory,* Vol. 25, No. 6, pp. 279-287.

28. Korn, G.A, and T.M. Korn, 1968, **Mathematical Handbook for Scientists and Engineers,** McGraw-Hill, New York, pp. 563-564.

29. Lockenvitz, A.E., J.B. Oliphint, W.C. Wilde, and J.M. Young, 1952, "Noncircular Cams and Gears," *Mechine Design,* Vol. 24, # 5, May, pp. 141-145.

30. Luck, K. and K.-H. Modler, 1995, "Synthesis Burmester Theory for Four-Bar-Band Mechanisms," *ASME, Journal of Mechanical Design,* Vol. 117, March, pp. 129-133.

31. Mabie, H. and C.F. Reinholtz, 1987, a, **Mechanisms and Dynamics of Machinery**, J. Wiley and Sons, New York.

32. Mabie, H. and C.F. Reinholtz, 1987, b, **Mechanisms and Dynamics of Machinery**, J. Wiley and Sons, New York. pp. 612-614.

33. MathWorks Inc., The, 1993, *Matlab 4.0*

34. Mathsoft Inc., 1994, *Mathcad 5.0,*

35. Mayourian, M. and F. Freudenstein, 1984, "The Development of an Atlas of the Kinematic Structures of Mechanisms," *ASME, Journal of Mechanisms, Transmissions, and Automation in Design,* Vol. 106, December, pp. 458-461.

36. McPhate, A.J., 1966, "Function Generation with Band Mechanisms," *Journal of Mechanisms,* Vol. 1, pp 85-94.

37. Miller, N.R. and D. Ross, 1980, "The Design of Variable-Ratio Chain Drives for Bicycles and Ergometers – Application to a Maximum Power Bicycle Drive," *ASME, Journal of Mechanical Design,* Vol. 105, October, pp. 711-717.

38. Molian, S. 1968, **The Design of Cam Mechanisms and Linkages,** American Elsevier Publishing, New York, pp 204-208.

39. Nautilus, 1993, *Next Generation,* sales brochure.

40. Norton, R.L., 1993, "A Brief History of Cams," *Modern Kinematics,* A.G. Erdman ed., John Wiley & Sons, New York, pp. 272-274.

41. Nathan, R.H., 1985, "A Constant Force Generation Mechanism," *Transactions of ASME,* Vol. 107, December, pp. 508-512.

42. Okada, T., 1986, "Optimization of Mechanisms for Force Generation by Using Pulleys and Spring," *The International Journal of Robotics Research,* Spring, pp. 508-512.

43. Olson, D.G., A.G. Erdman, and D.R. Riley, 1985, "A Systematic Procedure for Type Synthesis of Mechanisms with Literature Review," *Journal of Mechanisms and Machine Theory,* Vol. 20, No. 4, pp. 285-295.

44. Pracht, P., P. Minotti, and M. Dahan, 1987, "Synthesis and Balancing of Cam-Modulated Linkages," *ASME Advances in Design Automation* Vol. 10 # 2, ASME, New York, pp. 221-226.

45. Pryor, R.F., 1977, "Analytical Theories and Procedures for the Design of Cam-modulated Linkages," M.S. Thesis submitted to the Department of Mechanical Engineering, University of Florida.

46. Pryor, R.F, S.G. Dhande and G.N. Sandor, 1979, "On the Classification and Enumeration of Six-Link and Eight-Linkd Cam-Modulated Linkages," *Proceedings of the Fifth World Congress on Theory of Machines and Mechanisms*, Vol. 2, pp. 1315 - 1321.

47. Rankine, W.J.M., 1893, **A Manual of Machinery and Millwork**, Charles Griffin, London, pp. 185-190

48. Raghavan, M. and B. Roth, 1989, "On the Design of Manipulators for Applying Wrenches," *IEEE International Conference on Robotics and Automation,* Vol. 1, pp. 438-443.

49. Reuleaux, F., 1875, **A Kenematicts of Machery**, translation by Kennedy from German **Theoretische Kinematic**.

50. Roth, B., 1989, "Design and Kinematics for Force and Velocity Control of Manipulators and End-Effectors," *Robotics Science,* M. Brady, ed., MIT Press, pp. 459-475.

51. Rothbart, H.A., 1965, **CAMS, Design, Dynamics, and Accuracy,** J. Wiley and Sons, New York.

52. Sandor, G.N., 1993, "A Brief History of the First 40 Years of Modern American Kinematic Synthesis of Planar Mechanisms," *Modern Kinematics,* A.G. Erdman ed., John Wiley & Sons, New York, pp. 77-79.

53. Shigley, J.S., and L.D. Mitchell, 1993, **Mechanical Engineering Design,** McGraw-Hill, New York, pp.772-774.

54. Shooter, S.B., C.F. Reinholtz, and R.L. West, 1995, "A Unified Approach to Teaching Analytical Cam Design using Conjugate Geometry," accepted for publication in the *International Journal of Engineering Education.*

55. Shooter, S.B., P.H. Tidwell, and C.F. Reinholtz, 1994,"An Analytical Approach to Cam-Modulated Linkage Synthesis Using Conjugate Geometry," presented at the *ASME, 23rd Mechanisms Conference*, Minneapolis, MN.

56. Soper, R.R., M. Scardina, P.H.Tidwell, C.F. Reinholtz, and M.A. Lo Presti, 1995, "Closed-Form Synthesis of Force-Generating Planar Four-Bar Linkages," submitted to the *ASME Design Automation Conference*,

57. Streit, D.A. and B.J. Gilmore, 1989, " 'Perfect' Spring Equilibrators for Rotatable Bodies," *ASME, Journal of Mechanisms, Transmissions, and Automation in Design*, Vol. 111, December, pp. 451-458.

58. Swokowski, E.W., 1983, **Calculus with Analytic Geometry,** Prindle, Weber & Schmidt, Boston., pp. 611-615.

59. Svoboda, A., 1948, **Computing Mechanisms and Linkages,** McGraw-Hill, New York, pp. 20-23.

60. Tidwell, P.H., N. Bandukwala, S.G. Dhande, and C.F. Reinholtz, 1992, "Synthesis of Wrapping Cams," *Mechanism Design and Synthesis - Proceedings of the 1992 ASME Design Technical Conferences*, DE-Vol. 46, pp. 337-343.

61. Tidwell, P.H., N. Bandukwala, S.G. Dhande, C.F. Reinholtz, and G. Webb, 1994, "Synthesis of Wrapping Cams," *ASME, Journal of Mechanical Design*, Vol. 116, June, pp. 634-638.

62. Visual Basic, 1993, **Microsoft Visual Basic version 3.0,** developed for Microsoft by Cooper Software.

63. Webb, G.M., 1993, Interview with Greg Webb, Vice President of Engineering Nautilus.

    interview with Greg Webb, Vice President of Engineering Nautilus.

64. Yavne, R.O., 1948, "High Accuracy Contour Cams," *Product Engineering*, August, Vol. 19, # 8, pp.134-136.

# Vita

Paul H. Tidwell, II was born in Nashville, Tennessee on January 26, 1965. He graduated high school in 1983 from Montgomery Bell Academy, one of the best high schools in the south. He earned a bachelors degree with honors in mechanical engineering from Virginia Polytechnic Institute and State University in June 1987. He remained at Virginia Tech for a masters of science degree, defending it in June 1989. His primary interests are kinematics, design and teaching. He also enjoys investing, hang gliding, whitewater canoeing, and gardening. Paul plans to remain at Virginia Tech as a visiting faculty member, teaching strength of materials, mechanical design, and robotics.